**NAVAL SHIP RESEARCH AND DEVELOPMENT CENTER**

Bethesda, Maryland 20034



# FORCE AND MOMENT CHARACTERISTICS OF SIX HIGH-SPEED RUDDERS FOR USE ON HIGH-PERFORMANCE CRAFT

by

D. L. Gregory



APPROVED FOR PUBLIC RELEASE: DISTRIBUTION UNLIMITED



SHIP PERFORMANCE DEPARTMENT
RESEARCH AND DEVELOPMENT REPORT

November 1973

Report 4150

FORCE AND MOMENT CHARACTERISTICS OF SIX HIGH-SPEED RUDDERS FOR USE ON HIGH-PERFORMANCE CRAFT

The Naval Ship Research and Development Center is a U. S. Navy center for laboratory effort directed at achieving improved sea and air vehicles. It was formed in March 1967 by merging the David Taylor Model Basin at Carderock, Maryland with the Marine Engineering Laboratory at Annapolis, Maryland.

Naval Ship Research and Development Center
Bethesda, Md. 20034

## MAJOR NSRDC ORGANIZATIONAL COMPONENTS

*REPORT ORIGINATOR

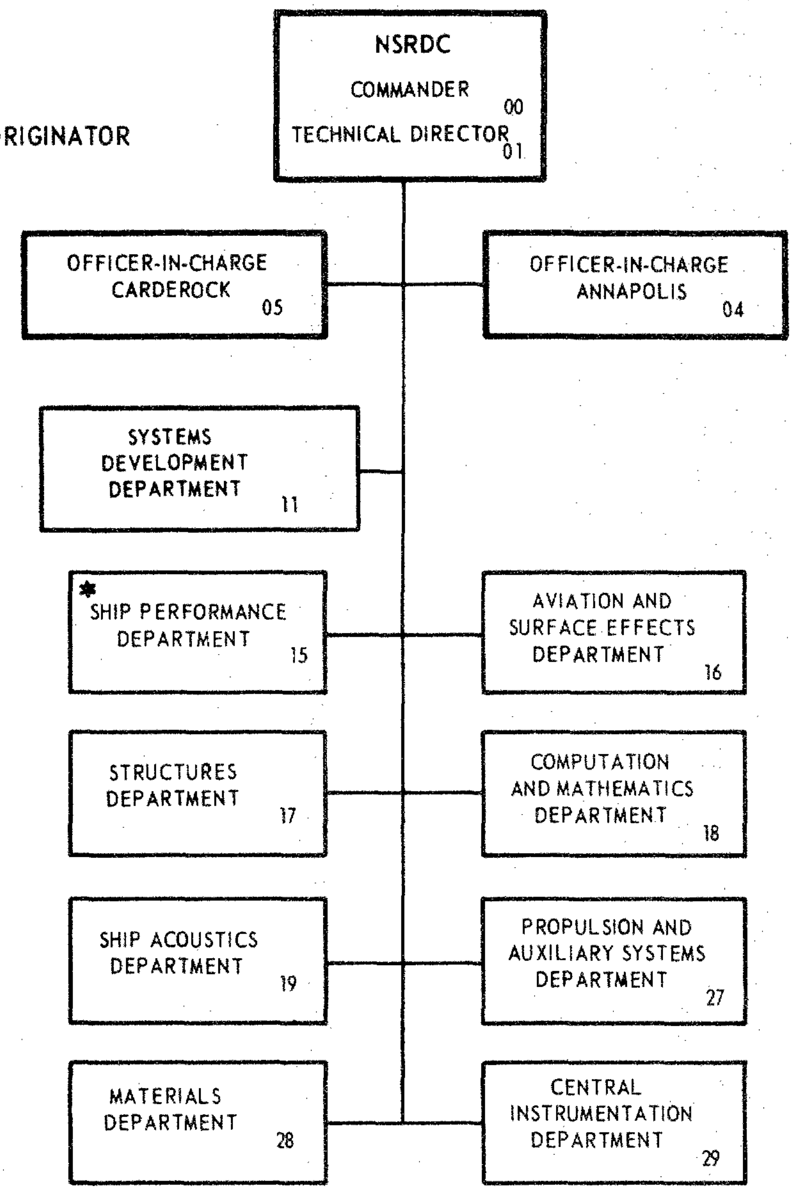

# NAVAL SHIP RESEARCH AND DEVELOPMENT CENTER

Bethesda, Maryland 20034



## FORCE AND MOMENT CHARACTERISTICS OF SIX HIGH-SPEED RUDDERS FOR USE ON HIGH-PERFORMANCE CRAFT

by

D. L. Gregory



APPROVED FOR PUBLIC RELEASE: DISTRIBUTION UNLIMITED



SHIP PERFORMANCE DEPARTMENT

RESEARCH AND DEVELOPMENT REPORT

November 1973

Report 4150

FORCE AND MOMENT CHARACTERISTICS OF SIX HIGH-SPEED RUDDERS FOR USE ON HIGH-PERFORMANCE CRAFT

DEPARTMENT OF THE NAVY
NAVAL SHIP RESEARCH AND DEVELOPMENT CENTER
BETHESDA, MD. 20034

# FORCE AND MOMENT CHARACTERISTICS OF SIX HIGH-SPEED RUDDERS FOR USE ON HIGH-PERFORMANCE CRAFT

by
D. L. Gregory



November 1973 Report 4150

TABLE OF CONTENTS



LIST OF FIGURES

NOTATION

| Symbol | Definition | Dimensions |
| --- | --- | --- |
| $A$ | Aspect ratio $b^2/S$ | |
| $b$ | Span measured perpendicular to the plane of the root section | feet |
| $\overline{C}$ | Mean geometric chord, $(\text{Chord}_{tip} + \text{Chord}_{root})/2$ | feet |
| $C_D$ | Drag coefficient, $D/\frac{1}{2}\rho S V^2$ | |
| $C_L$ | Lift coefficient, $L/\frac{1}{2}\rho S V^2$ | |
| $C_{M_{C/4}}$ | Torque coefficient about the mean geometric quarter chord, $M_C/\frac{1}{2}\rho S\overline{C}V^2$ | |
| $D$ | Drag parallel to flow | pound |
| $g$ | Acceleration due to gravity | feet per square second |
| $L$ | Lift normal to direction of flow | pound |
| $M_C$ | Rudder stock torque | pound-feet |
| $M_b$ | Rudder stock bending moment | pound-feet |
| $P_s$ | Static pressure | pounds per square foot |
| $P_v$ | Vapor pressure | pounds per square foot |
| $R_e$ | Reynolds number $V\overline{C}/\nu$ | |
| $S$ | Rudder planform area | square feet |

| Symbol | Definition | Dimensions |
|---|---|---|
| $V$ | Velocity of free stream | feet per second |
| $\alpha$ | Rudder angle (angle of attack) | degrees |
| $\nu$ | Kinematic viscosity | square feet per second |
| $\rho$ | Mass density | pound-square second per feet$^4$ |
| $\sigma$ | Cavitation number $(P_s - P_v)/\frac{1}{2}\rho V^2$ | |

## ABSTRACT

Six rudders with a geometric aspect ratio of 1.5 and widely varying section shapes were constructed to determine the effect of section shape on the cavitating performance of high-speed rudders. Experiments were conducted in the 24-in. variable-pressure water tunnel at cavitation indices between 4.0 and 0.5 and an angle of attack range from -5 to +35 deg. Section shape had little effect on the lift curve slope or on the maximum lift coefficient. However, the blunt base sections had substantially higher drag coefficients throughout the normal operating range of rudder angles. Rudder stock torque was significantly affected by section shape and cavitation index.

## ADMINISTRATIVE INFORMATION

This work was funded by Naval Ship Systems Command Code 03412B under Program Element 62512N, Project F35421, Subproject SF 35421006, Work Unit 1532-100.

## INTRODUCTION

The increasing cost of naval ships in the last decade has heightened interest in small high-performance craft, particularly for coastal and inshore warfare. The resultant demand for higher performance, better handling, and improved motion characteristics in a seaway has created a need for better predictions of speed and power, turning and maneuvering, and motion for such craft. This investigation of high-performance craft rudders is intended to provide much needed information on the force characteristics of rudders under the cavitating conditions experienced by high-performance craft. The purpose of this report is to aid in the design of rudders and steering gear and to provide rudder force characteristics for turning and maneuvering predictions.

A geometric aspect ratio of 1.5 was selected as representative of the current trend in rudder design. The two parameters chosen as variables were rudder section shape and cavitation number.

## THE RUDDER SERIES

Rudder profiles and typical section shapes for the six rudders tested are shown in Figures 1-6. The rudders were constructed of brass and polished to a smooth finish. They were fitted with 5/8-in. stainless steel stocks located at the mean quarter-chord point. All had a span of 7.5 in. and a mean chord of 5.0 in.; this gave a geometric aspect ratio of 1.5 and a projected area of approximately 37.5 $in^2$. Since Rudders 2, 3, and 5 had very thin leading edges, it was necessary to increase the width at the root so that it was thick enough to house the rudder stock. The normal rudder sections were maintained to a point 1 in. below the root on the model; above this point, the sections were thickened near the leading edge and were faired into the root section. This fairing is illustrated in Figures 2, 3, and 5.

## METHOD AND PROCEDURE

The experiments were conducted in the NSRDC 24-in. variable-pressure water tunnel.[1] The rudder angle was varied from -5 to +35 deg in 5-deg increments. The tunnel pressure and velocity were set to correspond to cavitation indices of 4.0, 2.0, 1.5, 1.0, and 0.5 for each rudder angle. A water velocity of 23 ft/sec for cavitation indices of 4.0 through 1.0 corresponds to a Reynolds number of approximately $1.02 \times 10^6$. The tunnel velocity was increased to 25 ft/sec for the 0.5 cavitation index, resulting in a small (about 8 percent) increase in Reynolds number for this condition compared to the other cavitation indices. The lower velocity at higher cavitation numbers was necessitated by the capacity of the force balance. Table 1 summarizes the experimental conditions. The cavitation patterns were observed and sketched for each condition.

[1]Brownell, W. F. and M. L. Miller, "Hydromechanics Cavitation Research Facilities and Techniques in Use at the David Taylor Model Basin," David Taylor Model Basin Report 1856 (Oct 1964).

TABLE 1 - SUMMARY OF EXPERIMENTAL CONDITIONS FOR EACH RUDDER

(Superscript numbers indicate the rudders on which cavitation first appeared for the indicated test condition)

| Angle of Attack deg | $\sigma$ | Tunnel Velocity ft/sec | Angle of Attack deg | $\sigma$ | Tunnel Velocity ft/sec |
|---|---|---|---|---|---|
| -5 | 4.0 | 23 | 20 | 4.0 | 23 |
| | 2.0 | ↓ | | $2.0^{1,2}$ | ↓ |
| | 1.5 | ↓ | | 1.5 | ↓ |
| | 1.0 | ↓ | | 1.0 | ↓ |
| | 0.5 | 25 | | 0.5 | 25 |
| 0 | 4.0 | 23 | 25 | 4.0 | 23 |
| | 2.0 | ↓ | | 2.0 | ↓ |
| | 1.5 | ↓ | | 1.5 | ↓ |
| | 1.0 | ↓ | | 1.0 | ↓ |
| | 0.5 | 25 | | 0.5 | 25 |
| 5 | 4.0 | 23 | 30 | 4.0 | 23 |
| | 2.0 | ↓ | | 2.0 | ↓ |
| | 1.5 | ↓ | | 1.5 | ↓ |
| | $1.0^{3,4,6}$ | ↓ | | 1.0 | ↓ |
| | $0.5^{2-6}$ | 25 | | 0.5 | 25 |
| 10 | 4.0 | 23 | 35 | 4.0 | 23 |
| | $2.0^{3-6}$ | ↓ | | 2.0 | ↓ |
| | $1.5^{2-6}$ | ↓ | | 1.5 | ↓ |
| | $1.0^{5}$ | ↓ | | 1.0 | ↓ |
| | $0.5^{1}$ | 25 | | 0.5 | 25 |
| 15 | 4.0 | 23 | | | |
| | $2.0^{2}$ | ↓ | | | |
| | $1.5^{1}$ | ↓ | | | |
| | $1.0^{1}$ | ↓ | | | |
| | 0.5 | 25 | | | |

The rudders were tested below an 8.0-in. × 21.5-in. aluminum plate with a gap of approximately $0.005\overline{C}$ between the top of the rudder and the plate. Forces and moments were measured with four 2-in. modular force gages and with a transmission dynamometer mounted above the plate and housed in a faired strut. A schematic diagram of the measurement system is shown in Figure 7. All gages were calibrated individually, assembled in the system, and then calibrated as a total system. Lift and drag forces are accurate to ±0.5 lb, rudder stock torque to ±0.5 in-lb, and rudder stock bending moments to ±1.0 in-lb. Lift forces on the model rudders varied from 0 to 150 lb, and the drag varied from near zero to approximately 75 lb. Maximum rudder stock torques were in the order of 100 in-lb.

All data were reduced to nondimensional coefficient forms compatible with the coefficients presented by Whicker and Fehlner.[2]

## RESULTS AND DISCUSSION

Figures 8-13 show representative cavitation patterns for the six rudders, and Figures 14-19 indicate their lift, drag, and torque coefficients. Figure 20 presents a comparison of the lift and drag coefficients of the six rudders at $\sigma = 4.0$ and 0.5. It is apparent from Figures 14-19 that the NACA 0015 section rudder (Rudder 1) was the only one that showed any appreciable loss in maximum lift coefficient for cavitation indices of 1.0 or greater. This deterioration occurred mainly at rudder angles greater than 15 deg; such angles are probably beyond the normal operating range of a high-speed rudder. The effective angle of attack of a rudder operating on a real craft will generally be somewhat less than the rudder angle once the craft starts to turn.

The lift curve slopes ($dC_L/d\alpha$) of the six rudders for $\sigma = 4.0$ and 1.0 did not vary significantly from one another for angles of attack less

[2] Whicker, L. F. and L. F. Fehlner, "Free-Stream Characteristics of a Family of Low-Aspect Ratio, All-Movable Control Surfaces for Application to Ship Design," David Taylor Model Basin Report 933 (May 1958).

than 15 deg. The maximum lift occurred between 22 and 25 deg for all rudders except Rudder 6 where the maximum was at approximately 27 deg. Rudders 2, 3, and 5, which had their maximum thickness at the trailing edge, had both higher lift slope and higher maximum lift coefficients than the other three.

The flat plate had the lowest maximum lift coefficient; however, the lift slope was equal to the NACA 0015 section up to an angle of attack of 15 deg. For angles less than 25 deg, the drag of the NACA 0015 section shape rudder was substantially less than that of any of the other five rudders tested. If the lift to drag ratio of a rudder is used as a figure of merit, then the NACA 0015 rudder performed best. This can be seen from Figure 21 which shows a comparison of the L/D ratios of the six rudders for $\sigma = 4.0$ and 0.5. The NACA 0015 rudder exhibited high negative torque on the rudder stock over a wide range of angles. This means that once the rudder started to turn, it would turn further on its own until it reached a high angle of attack. This can be rectified by increasing the sweep angle or moving the rudder stock forward.

Considering manufacturing costs, particularly on a craft of medium speed, the flat plate rudder is probably the best choice. The drag coefficient lies about midway between the high and the low values obtained with this rudder series. The drag coefficient of the flat plate rudder at 0-deg angle of attack could probably be reduced by fairing the trailing edge with straight line sections so that the trailing edge has a 20- to 30-deg included angle.

At high speed ($\sigma = 0.5$), the lift curve slope for the NACA 0015 section was equal to the noncavitating lift curve slope up to approximately 10 deg. Beyond a 10-deg angle of attack, the lift slope dropped sharply and the maximum lift coefficient was in the order of 60 to 70 percent of the maximum lift coefficient developed at cavitation indices of 1.0 and larger. At cavitation indices of 0.5 and below, the NACA 0015 rudder did not perform as well as in the 1.0 to 4.0 range. The lift on this rudder started to drop rather drastically at approximately 18 deg and continued until it reached a minimum at approximately 24 deg. At low angles of attack, however, the drag was still substantially lower than that of any of the other sections tested. At $\sigma = 0.5$, the performance of the flat

plate rudder again suggested that this rudder is a reasonably good selection. However, it is likely that under cavitation conditions, both rudders will have cavitation erosion problems. At $\sigma = 0.5$ and lower, Rudder 2 (the parabolic section) is probably the best choice. Its thicker leading edge will be less subject to damage than Rudders 3 and 5 and it does not require as much thickening to provide adequate strength in the area of the rudder stock. The parabolic section was less susceptible to cavitation erosion damage than the flat plate or the NACA 0015 section.

The effect of cavitation on the lift, drag, and rudder stock torque characteristics has already been discussed. It is interesting to note that cavitation actually began at considerably lower (simulated) speeds than the speed where any detrimental effects in performance were first observed. Unfortunately, cavitation inception studies on these rudders were not conducted; however, cavitation patterns were observed at each test condition. The summary of experimental conditions (Table 1) indicates the point at which cavitation was first observed for each rudder. Since both the cavitation number and the angle of attack were varied in discrete increments, the actual cavitation inception point will probably occur at a higher value of $\sigma$ than indicated in Table 1. It is shown, for example, that cavitation was first present on Rudder 3 at a 5-deg angle of attack and $\sigma = 1.0$. Since no cavitation was indicated at $\sigma = 1.5$, it can be assumed that the actual inception point for Rudder 3 at a 5-deg angle of attack was between $\sigma = 1.5$ and 1.0.

The stepped rudder (Rudder 6 shown in Figure 6) was designed to operate with the after portion unwetted at high speeds, in order to reduce the drag, but flow separation did not seem to take place. At $\sigma = 0.5$ and a 0-deg angle of attack, a very small cavity in the order of 1/8 in. long formed behind the step. At higher sigma values there was no evidence of cavitation at the step and the drag results do not indicate that flow separation occurred. Since this rudder was designed to operate very near the surface where there is a distinct possibility of ventilation, it was decided to try to ventilate the rudder by injecting air at the step. Air was injected by leading a tube (inside diameter of approximately 3/32 in.) from the bottom of the tunnel. Several locations of the air tube as well as several angles of attack on the rudder were investigated. It was not

possible to ventilate the rudder at the step in this manner, providing further evidence that flow separation was not present. When ventilation did occur, the rudder ventilated from the leading edge. Thus, it was not possible to obtain the characteristics of this rudder with the afterbody unwetted. If it does not ventilate, Rudder 6 offers no significant advantage over Rudders 2, 3, and 5. These experiments are not conclusive proof that the rudder will not ventilate under full-scale conditions.

For this series of rudders, the spanwise center of pressure was between 40 to 50 percent of the span from the root. For the purpose of sizing the rudder stock, the spanwise center of pressure may be assumed to be 0.45b from the root. The rudder stock bending moment may then be calculated as

$$M_B = \sqrt{L^2 + D^2} \times 0.45b$$

## COMPARISON WITH OTHER EXPERIMENTAL DATA

The lift and drag coefficients for Rudder 1 (NACA 0015) obtained from this series of experiments are compared in Figures 22 and 23 with data for similar rudders.[2, 3] The water tunnel results from Kerwin et al.[3] are for a rudder with an NACA 66 section of aspect ratio 1.4; they agreed quite well in both lift and drag and with the results obtained here for angles of attack of less than 20 deg. The lift slope of the NACA 66 rudder was slightly lower than for Rudder 1 of the present study; this is what one would expect since the aspect ratio was lower. Figure 23 shows that the drag characteristics of these two rudders began to deviate considerably at angles of attack larger than 20 deg. This lack of agreement between the drag coefficients is due to the difference in stall angles. The lift breakdown occurred at 20 deg on the NACA 66 rudder and at 23 deg on the NACA 0015 rudder.

[3]Kerwin, J. E. et al., "An Experimental Study of a Series of Flapped Rudders," Mass. Inst. Technol. Report 71-19 (Jul 1971).

The results of the wind tunnel lift data[2] corrected to a Reynolds number of $1.02 \times 10^6$ agreed reasonably well with water tunnel data from the present study. The lift curve slope $\left(dC_L/d\alpha\right)$ obtained in the wind tunnel was 0.0506 compared to 0.0467 for the water tunnel studies. This represents a difference of approximately 10 percent in the lift curve slope. The maximum lift coefficient, however, was about the same for both series of experiments. The drag data in Figure 23 show about a 10-percent difference between the wind tunnel and water tunnel experiments. No corrections for Reynolds number effects were made to the wind tunnel data for the drag coefficient because Whicker and Fehlner[2] had indicated that a change in Reynolds number from $1.02 \times 10^6$ to $2.26 \times 10^6$ did not significantly affect the drag.

The agreement among the three experiments is quite reasonable. The data presented in this paper are therefore considered sufficiently accurate for use in designing rudders for high-performance craft.

## CONCLUSIONS

1. Rudder section shape has little effect on rudder effectiveness (lift curve slope) for angles less than 15 deg.

2. For cavitation number values of 1.0 and larger, Rudder 1 (NACA 0015 section) has the highest lift to drag ratio and the lowest drag.

3. For low- and medium-speed rudders, the flat plate rudder is a good compromise between cost and performance.

4. For high-speed application ($\sigma = 0.5$ or lower), the parabolic section (Rudder 2) appears to be the best choice.

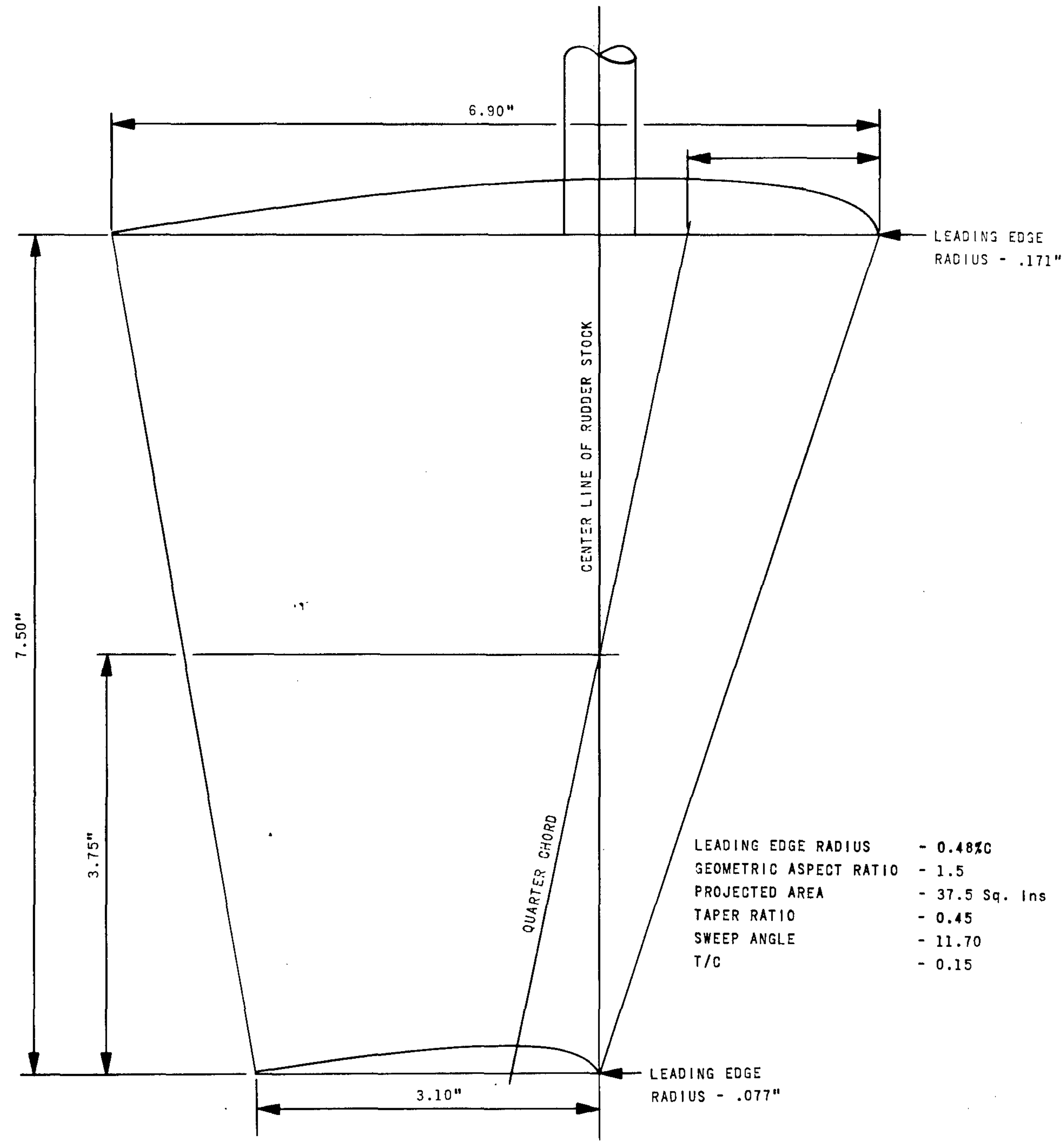


Figure 1 - Planform and Section Details of Rudder 1

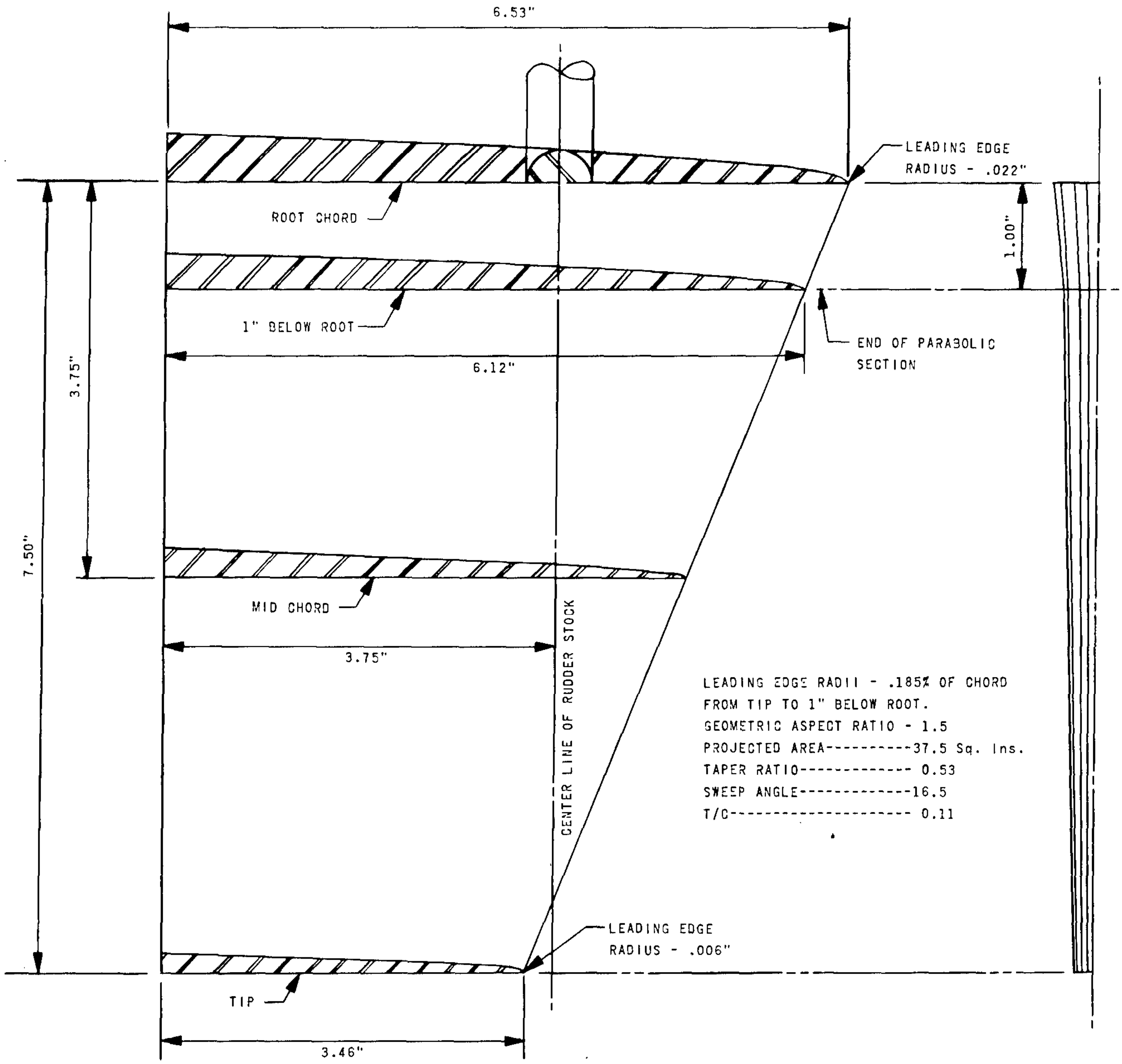


Figure 2 - Planform and Section Details of Rudder 2

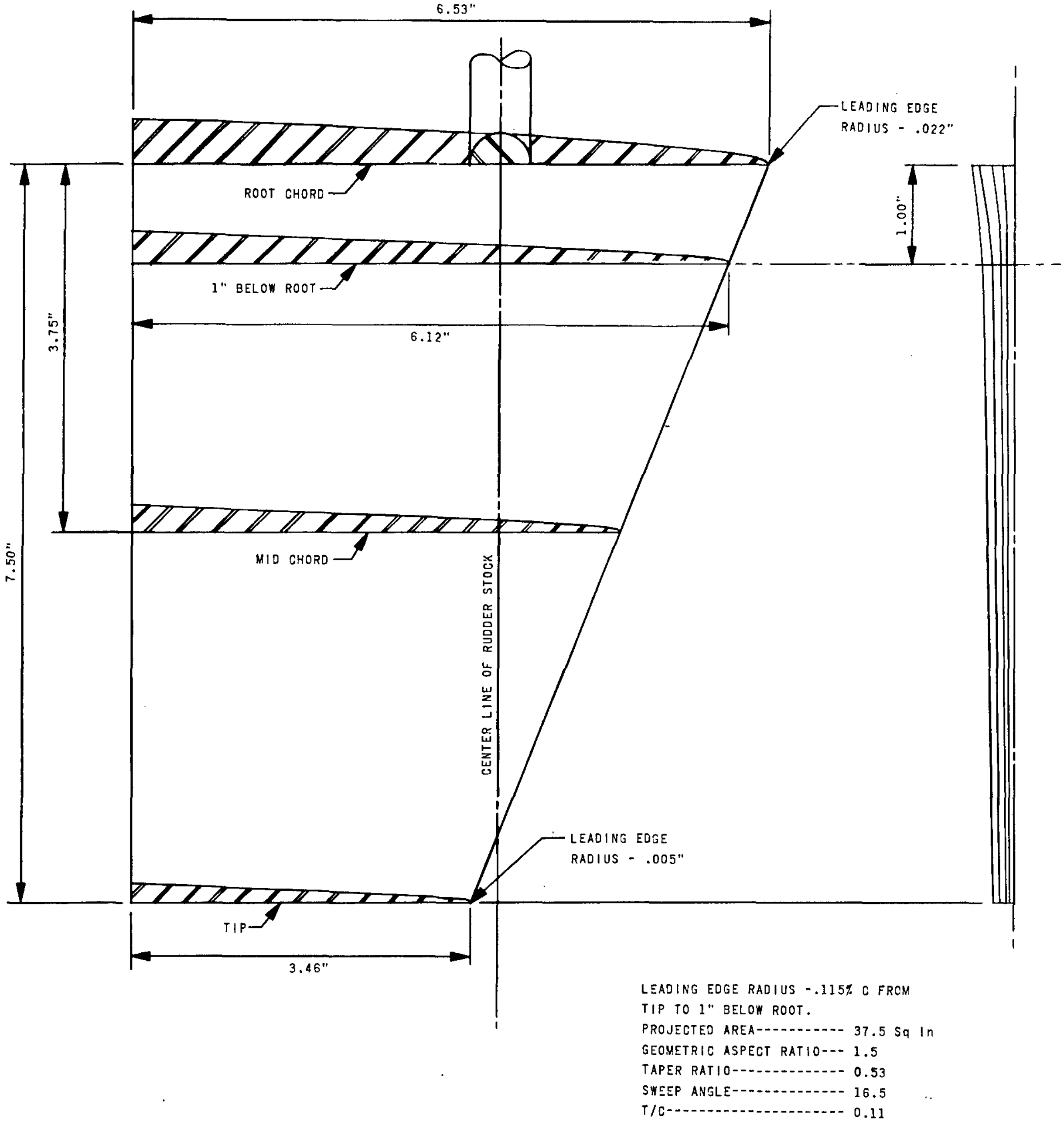


Figure 3 - Planform and Section Details of Rudder 3

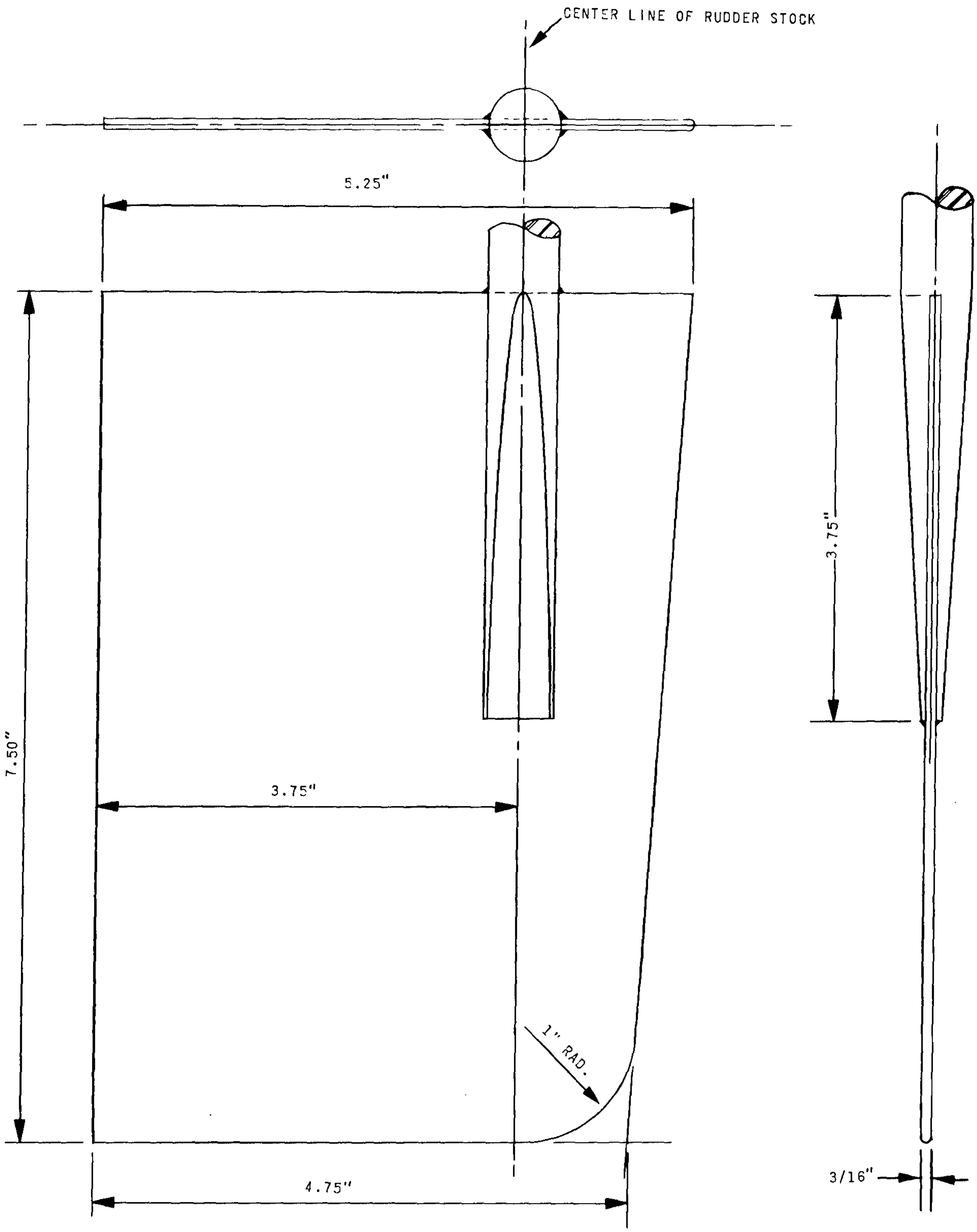


Figure 4 - Planform and Section Details of Rudder 4

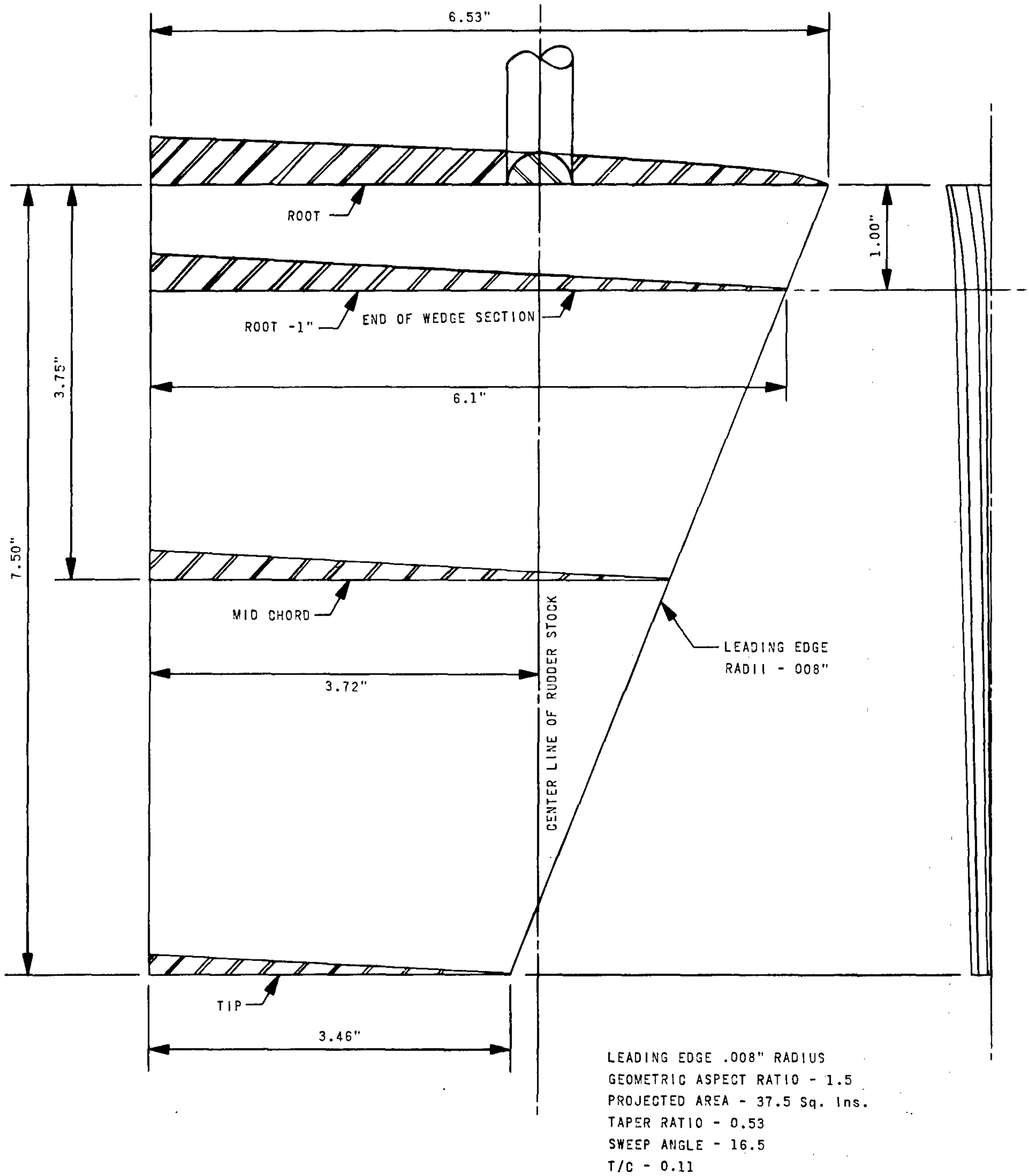


Figure 5 - Planform and Section Details of Rudder 5

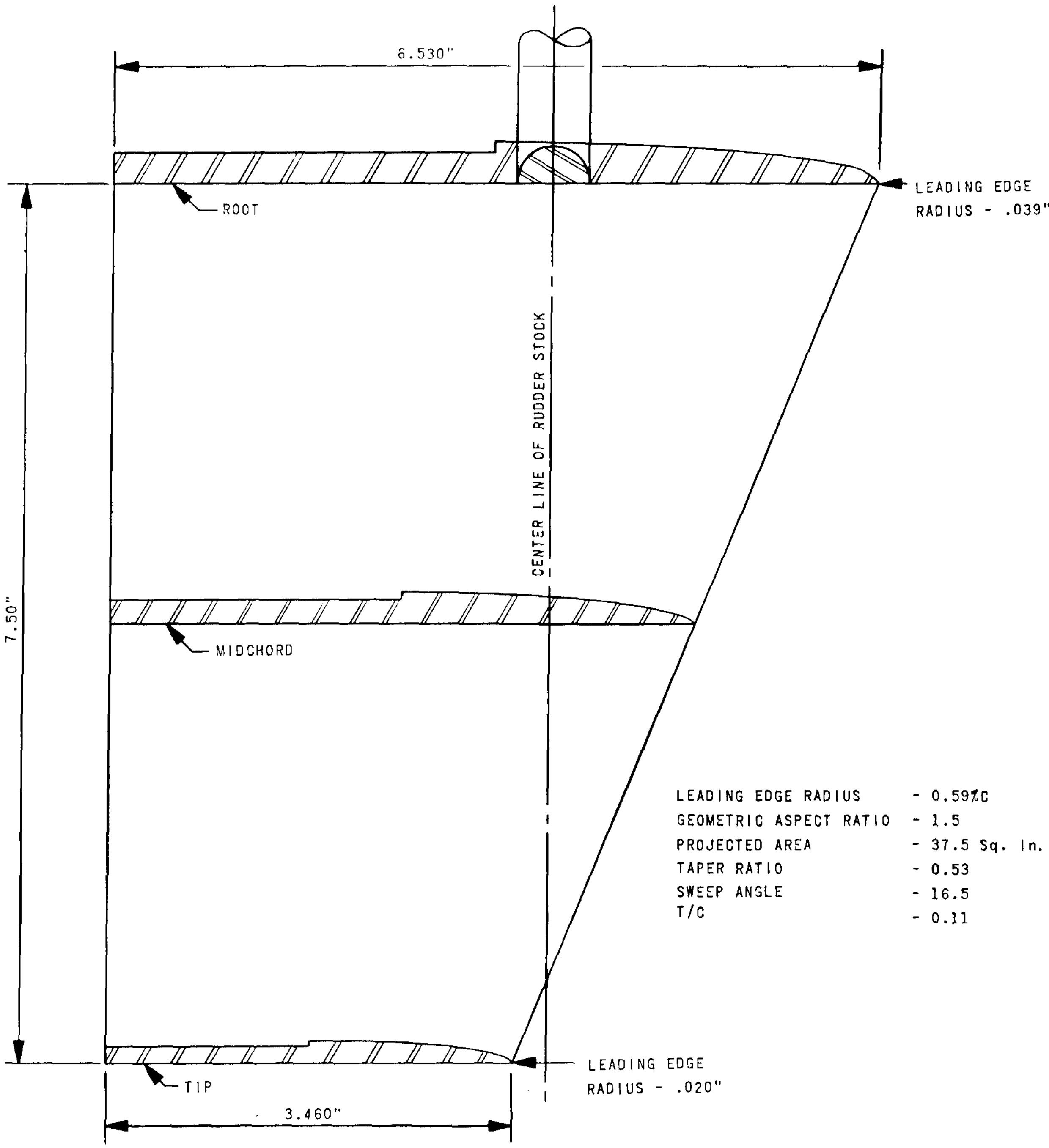


Figure 6 - Planform and Section Details of Rudder 6

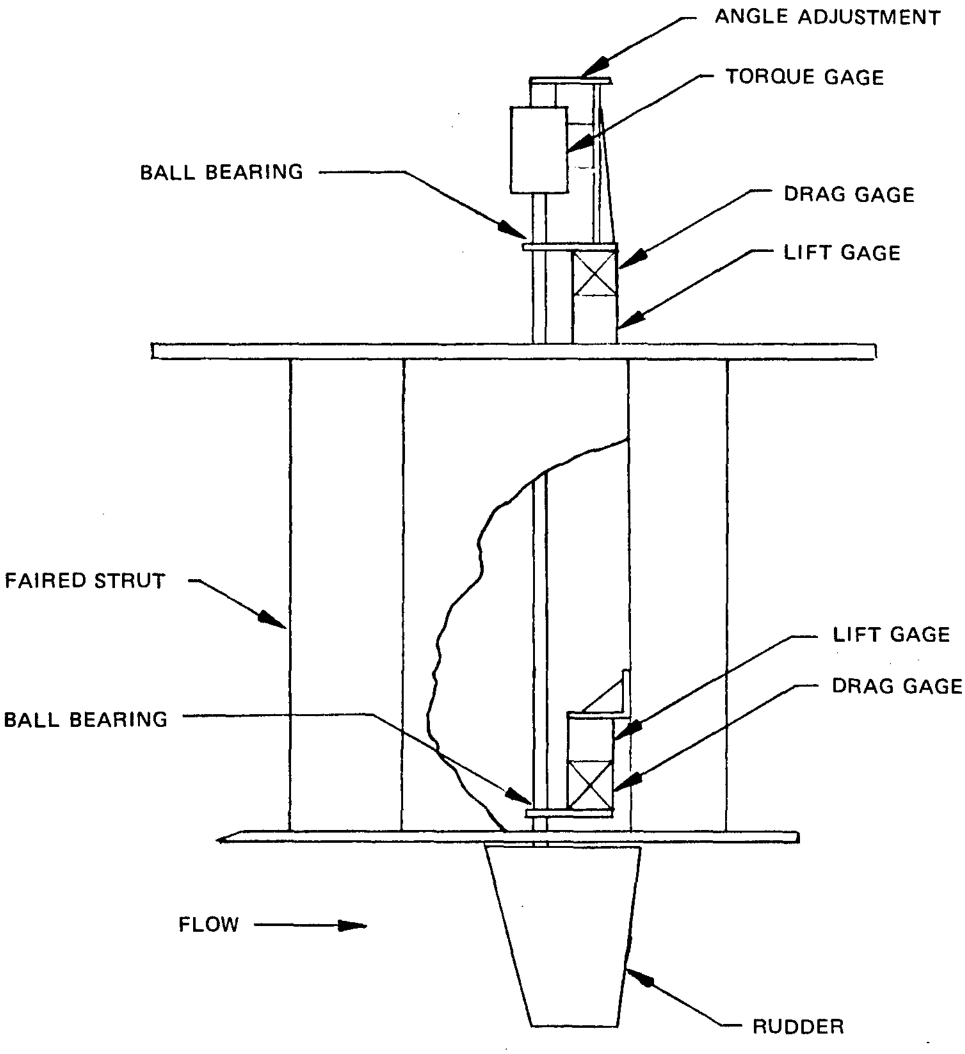


Figure 7 - Details of the Rudder Force Dynamometer Used to Make Force Measurements in the 24-Inch Variable-Pressure Water Tunnel

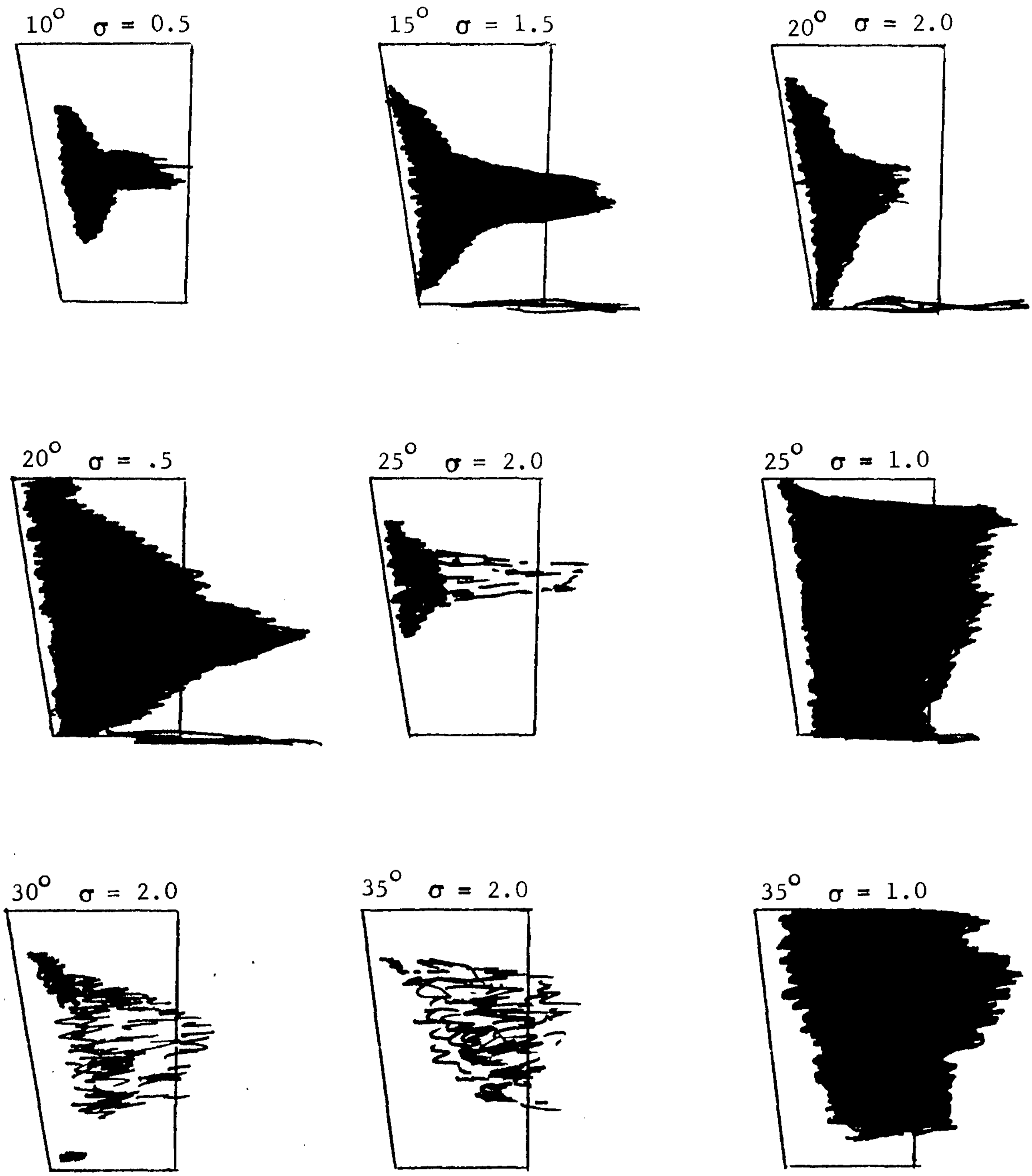


Figure 8 - Representative Cavitation Patterns on Rudder 1

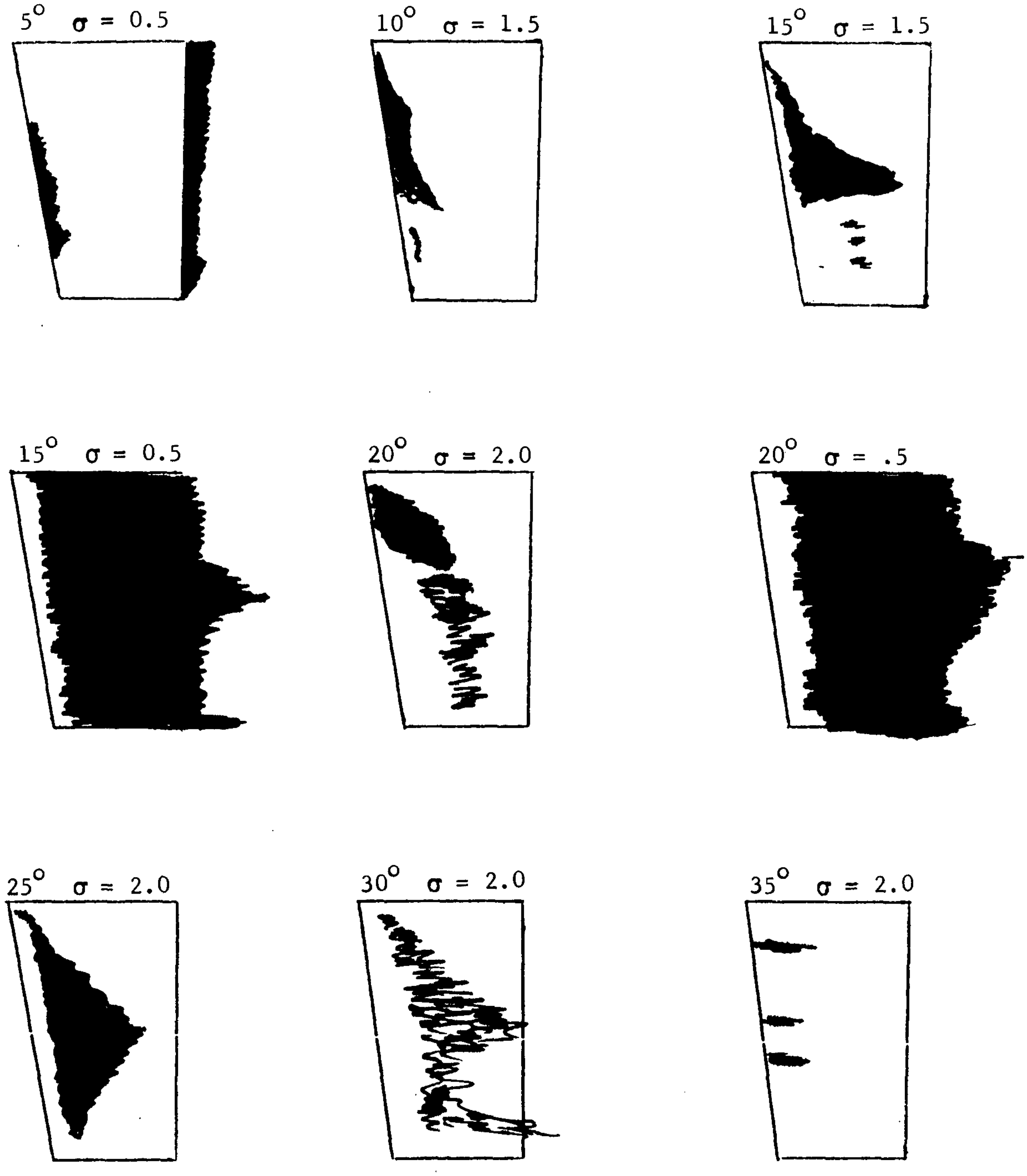


Figure 9 - Representative Cavitation Patterns on Rudder 2

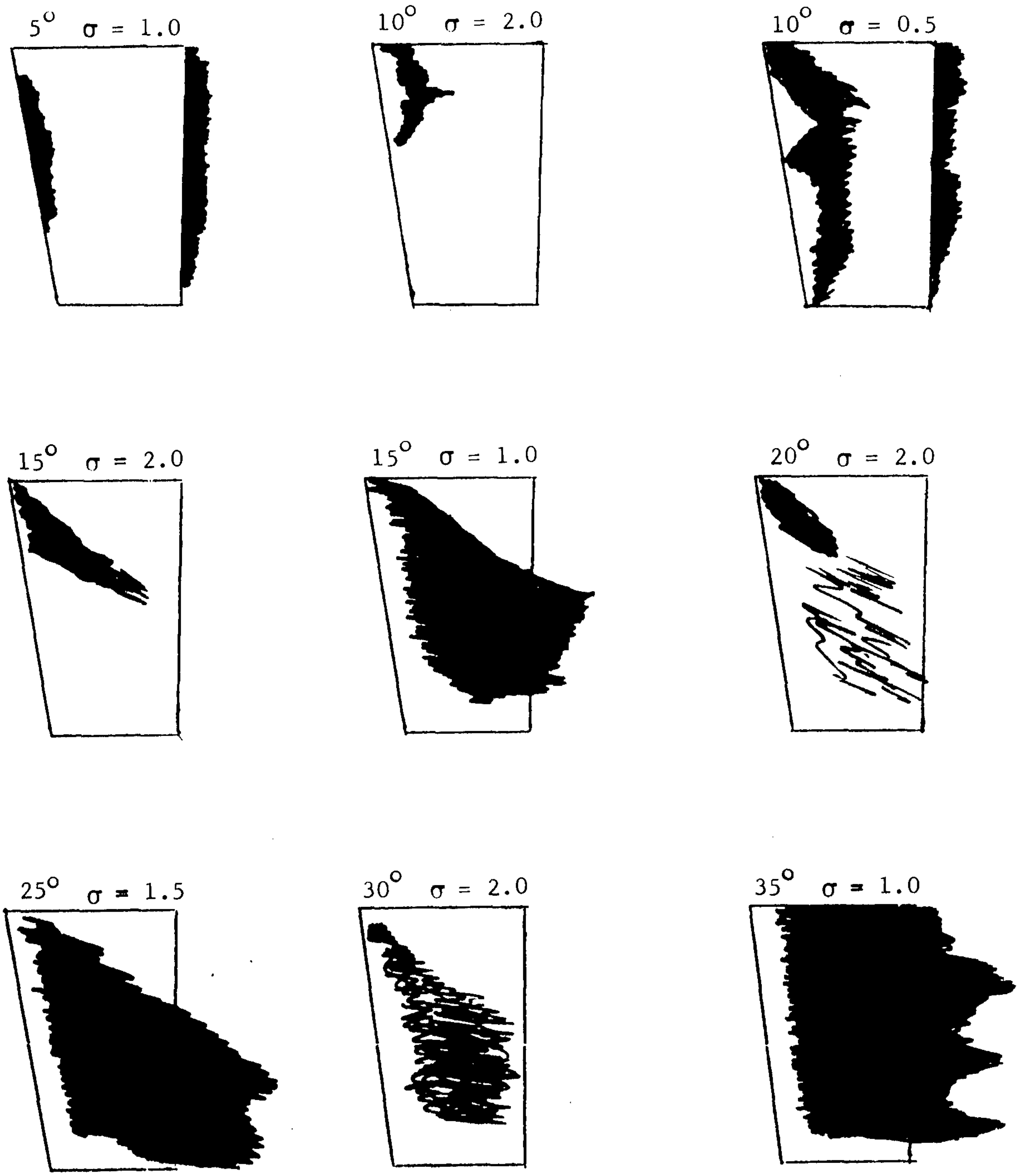


Figure 10 - Representative Cavitation Patterns on Rudder 3

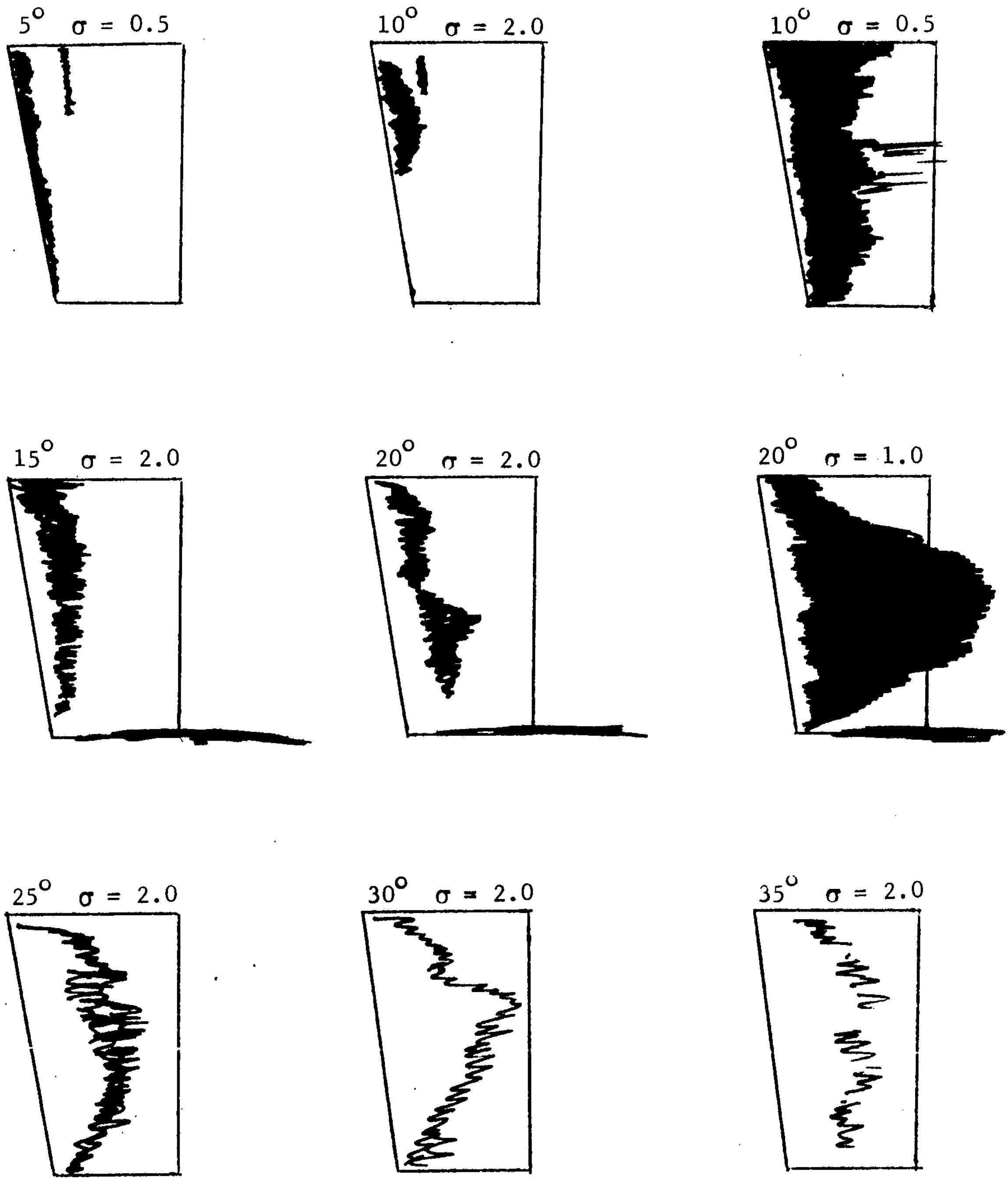


Figure 11 - Representative Cavitation Patterns on Rudder 4

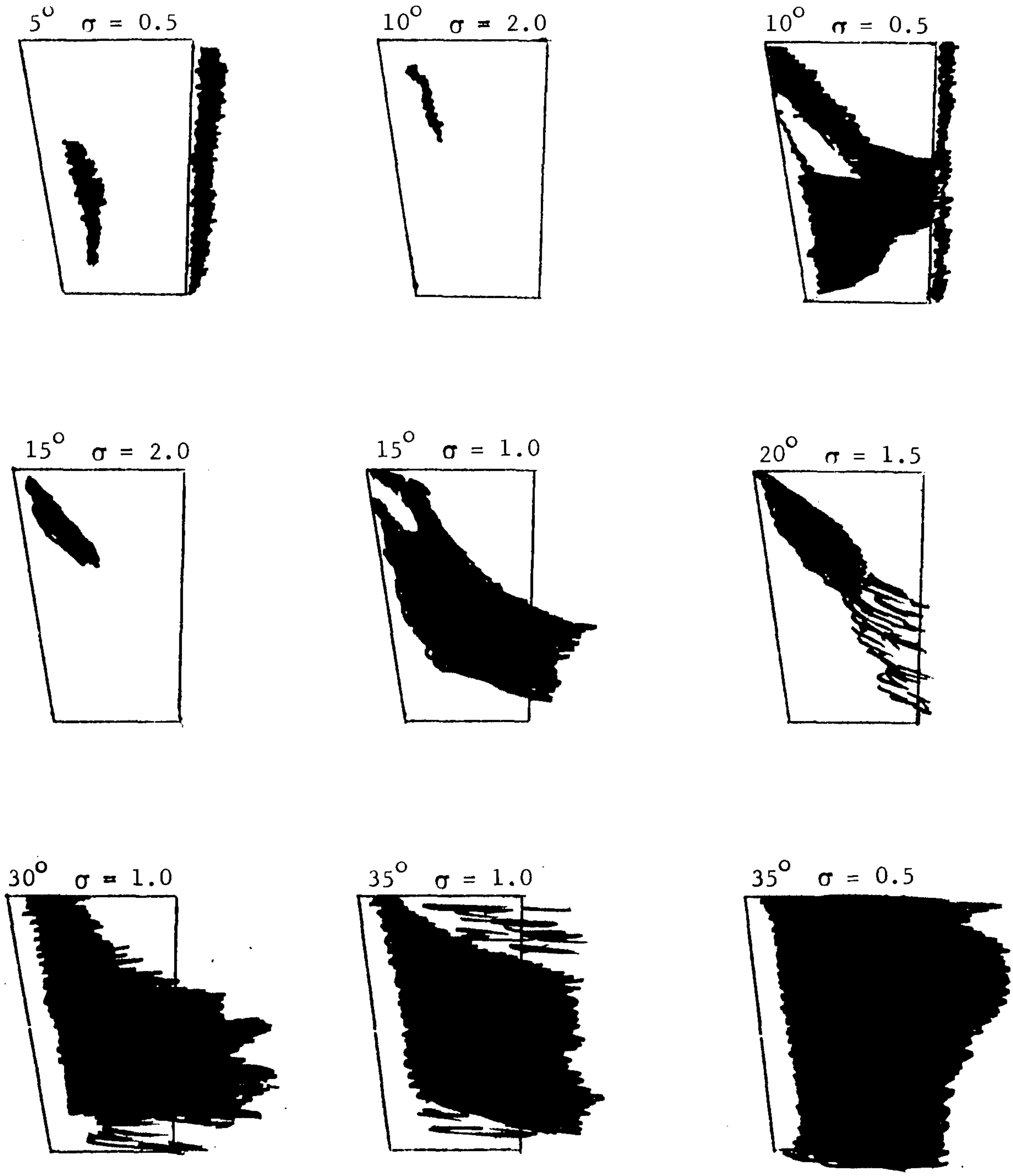


Figure 12 - Representative Cavitation Patterns on Rudder 5

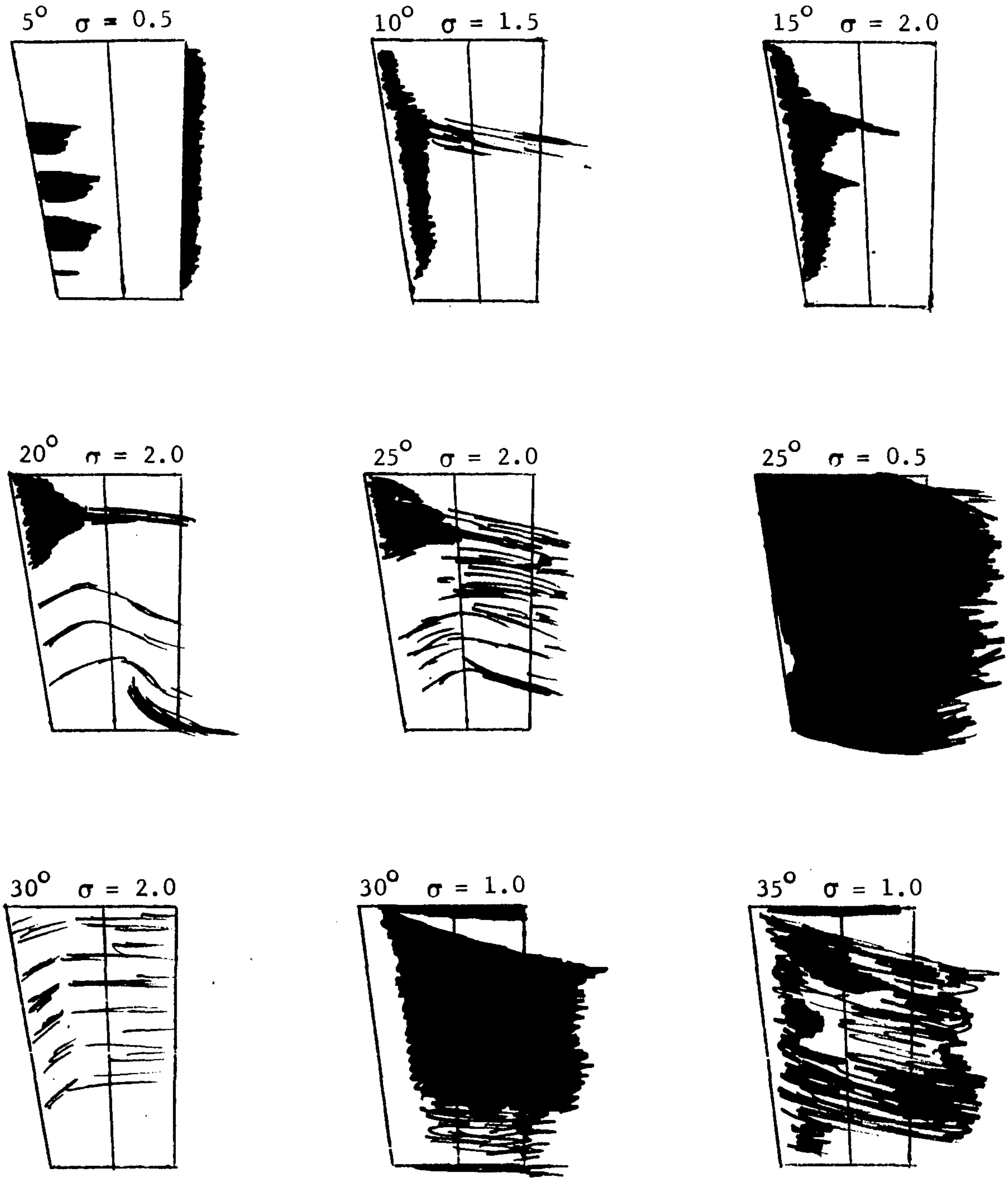


Figure 13 - Representative Cavitation Patterns on Rudder 6

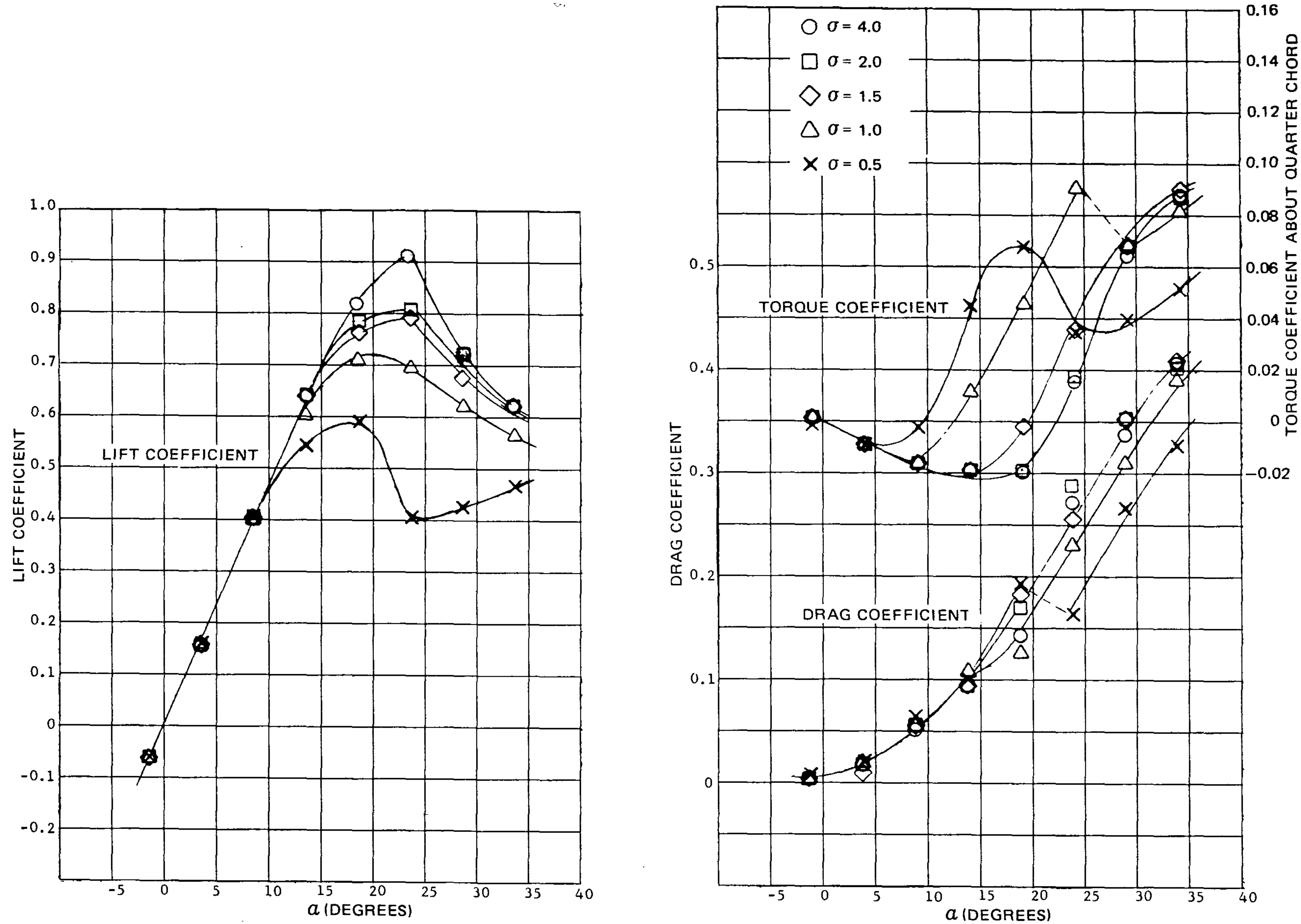


Figure 14 - Force and Moment Coefficients Measured on Rudder 1 at Several Rudder Angles and Cavitation Indices

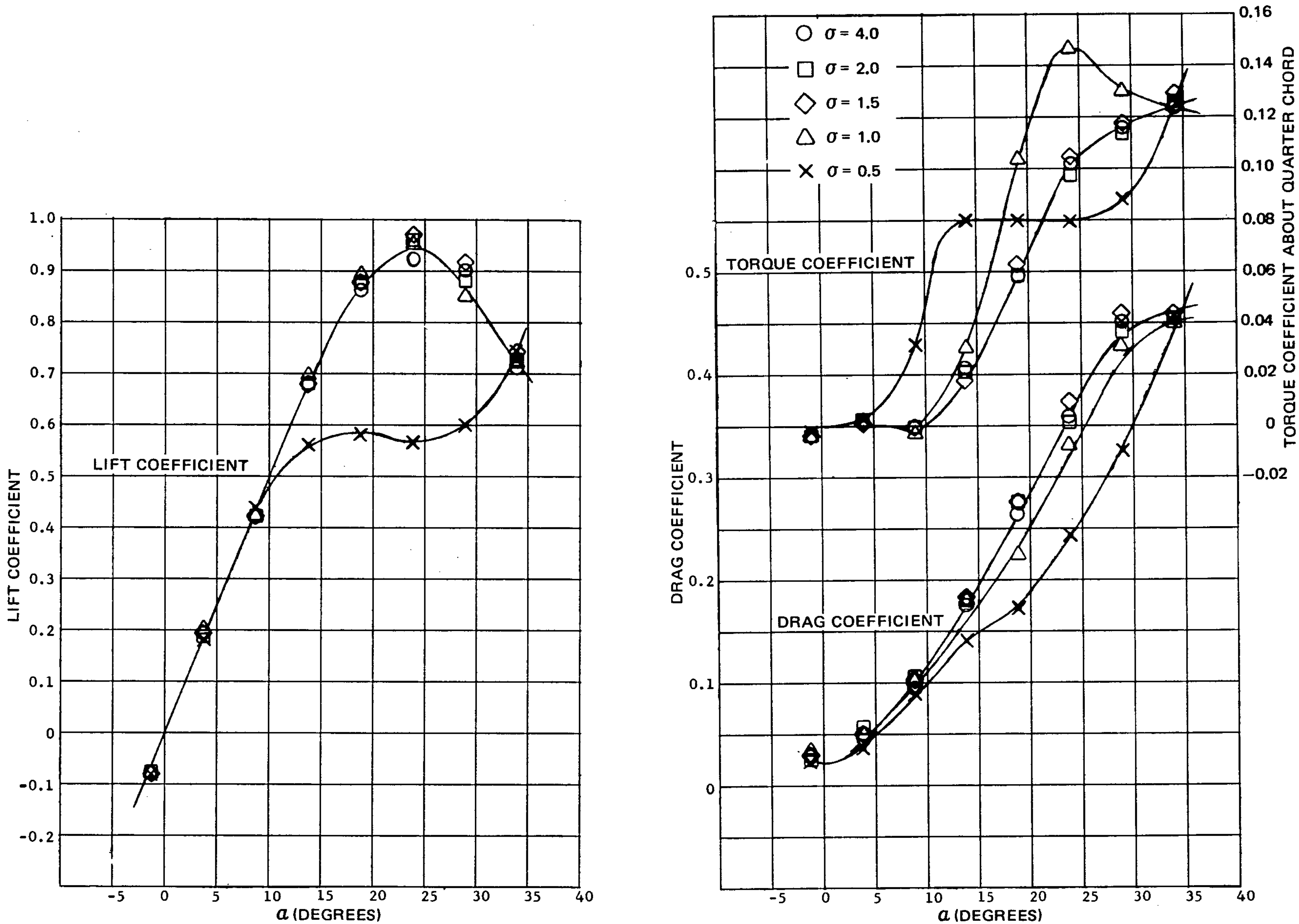


Figure 15 - Force and Moment Coefficients Measured on Rudder 2 at Several Rudder Angles and Cavitation Indices

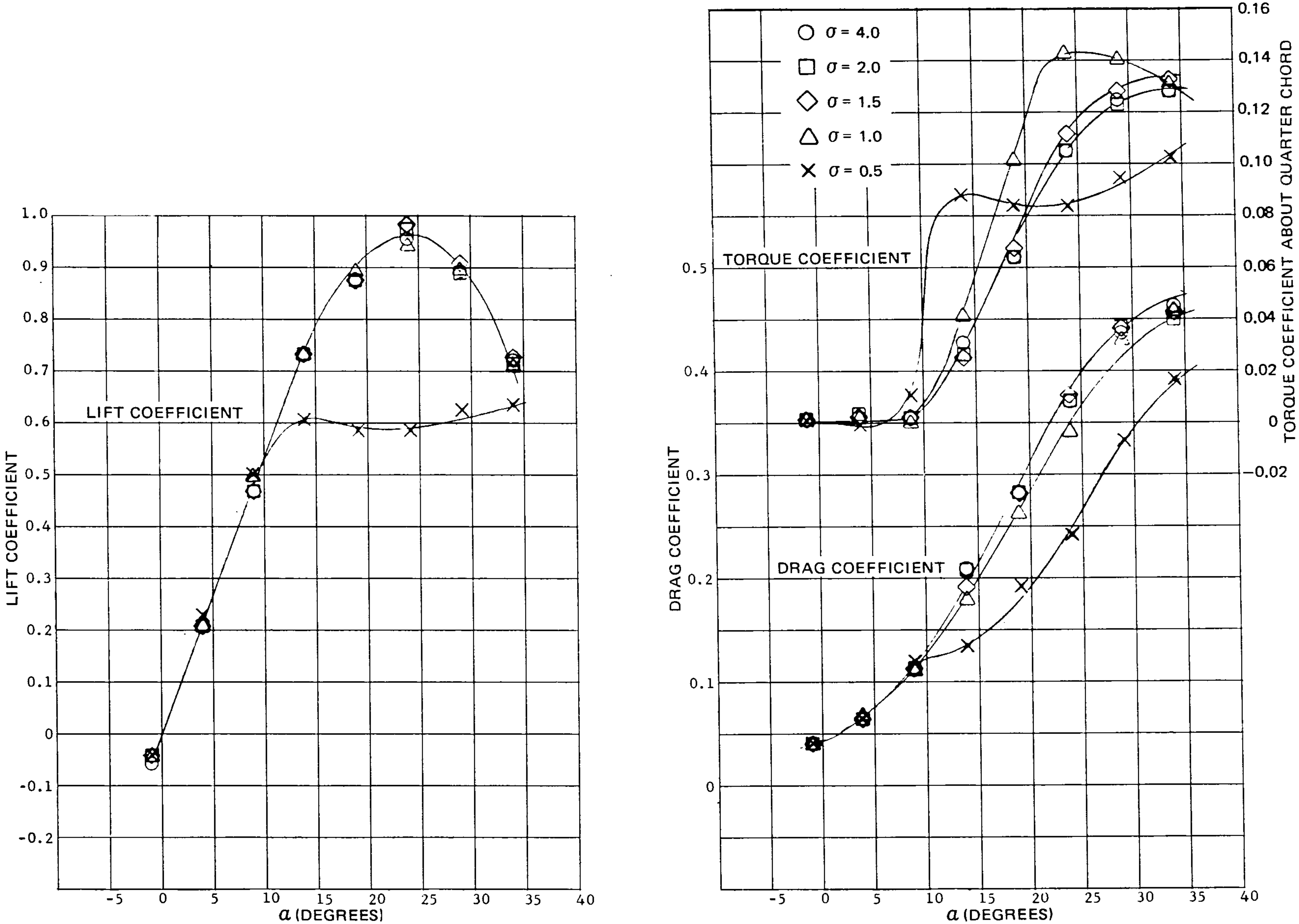


Figure 16 - Force and Moment Coefficients Measured on Rudder 3 at Several Rudder Angles and Cavitation Indices

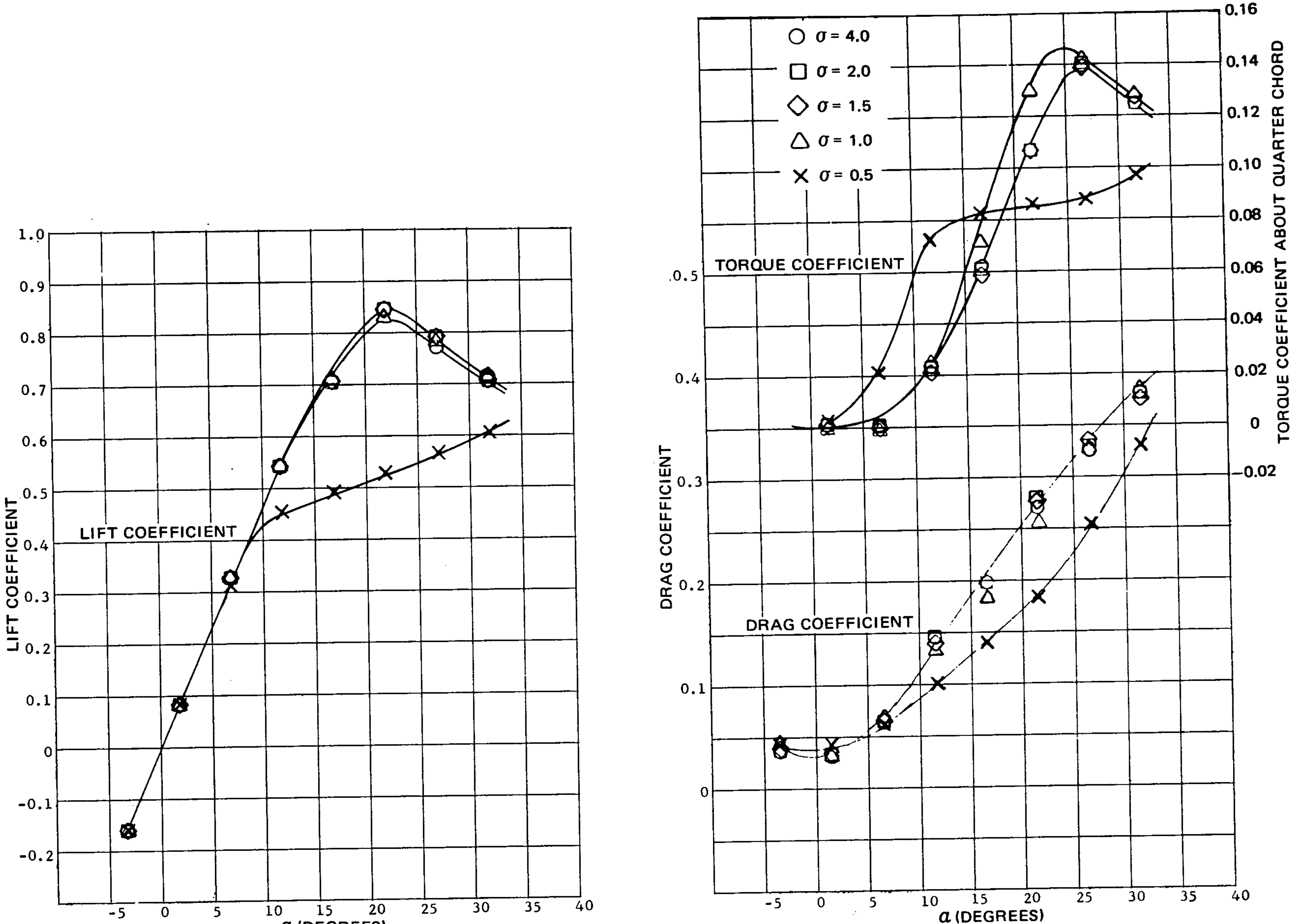


Figure 17 - Force and Moment Coefficients Measured on Rudder 4 at Several Rudder Angles and Cavitation Indices

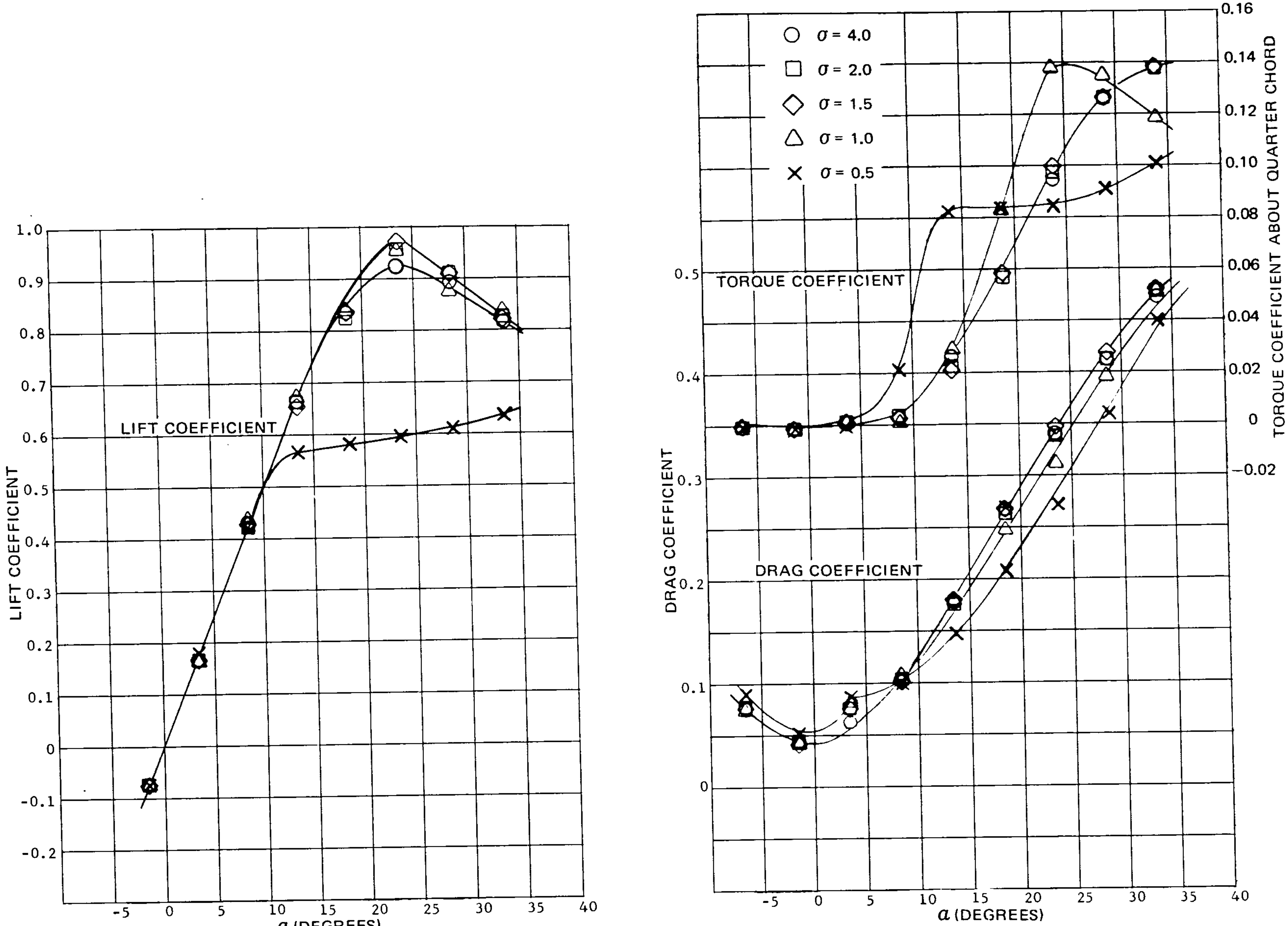


Figure 18 - Force and Moment Coefficients Measured on Rudder 5 at Several Rudder Angles and Cavitation Indices

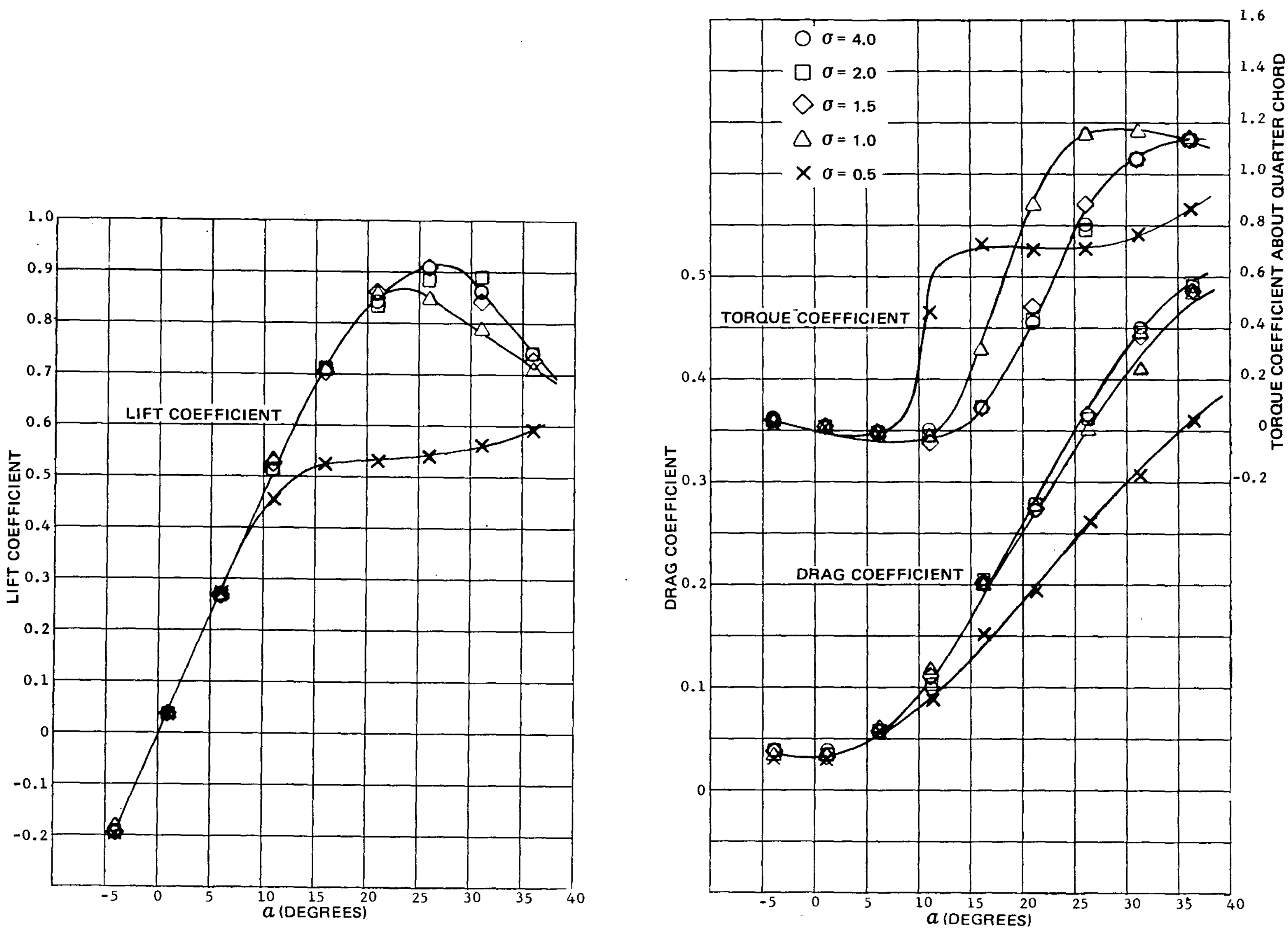


Figure 19 - Force and Moment Coefficients Measured on Rudder 6 at Several Rudder Angles and Cavitation Indices

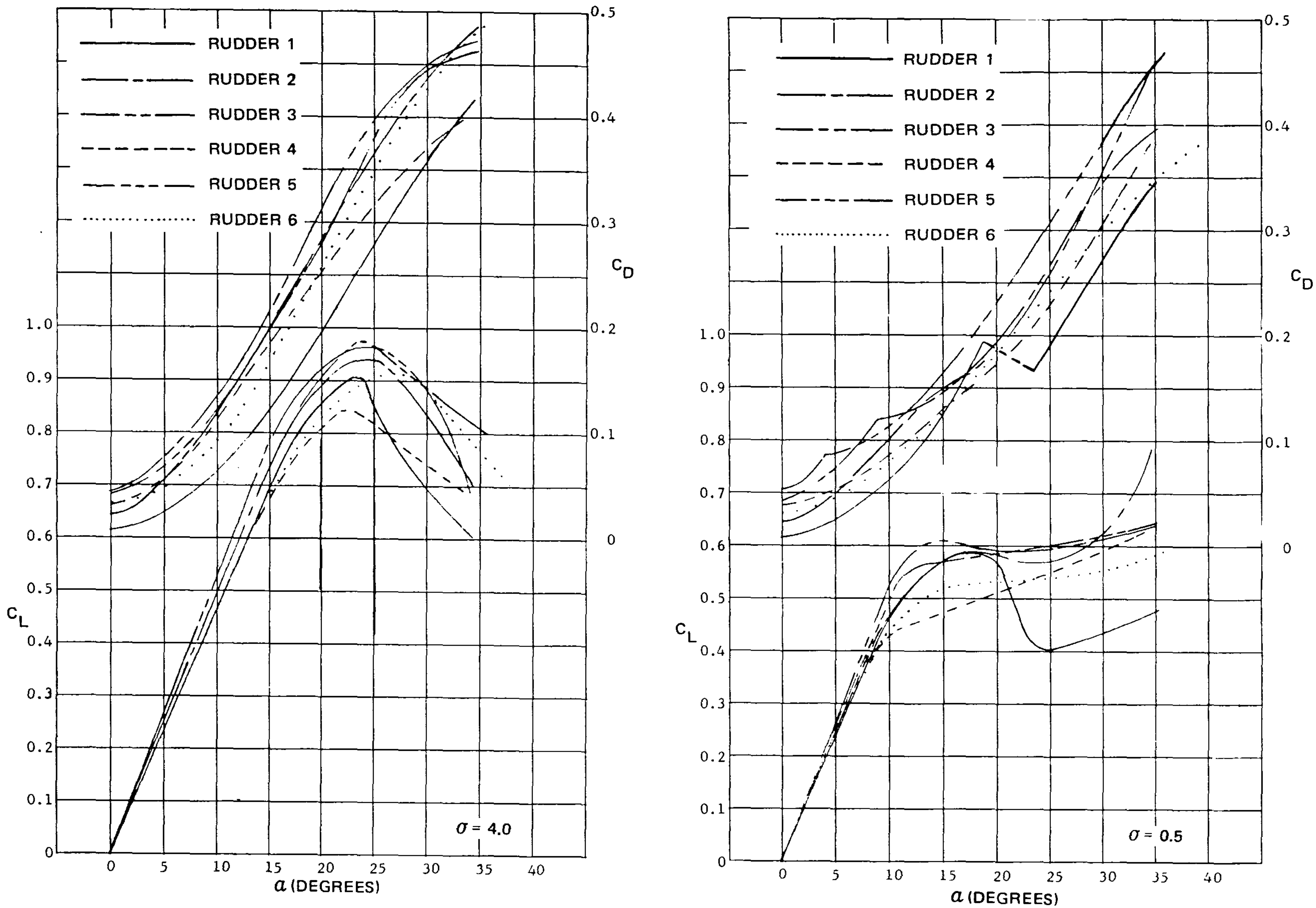


Figure 20 - Comparison of Lift and Drag Coefficients of Rudders 1-6 at Cavitation Indices of 4.0 and 0.5

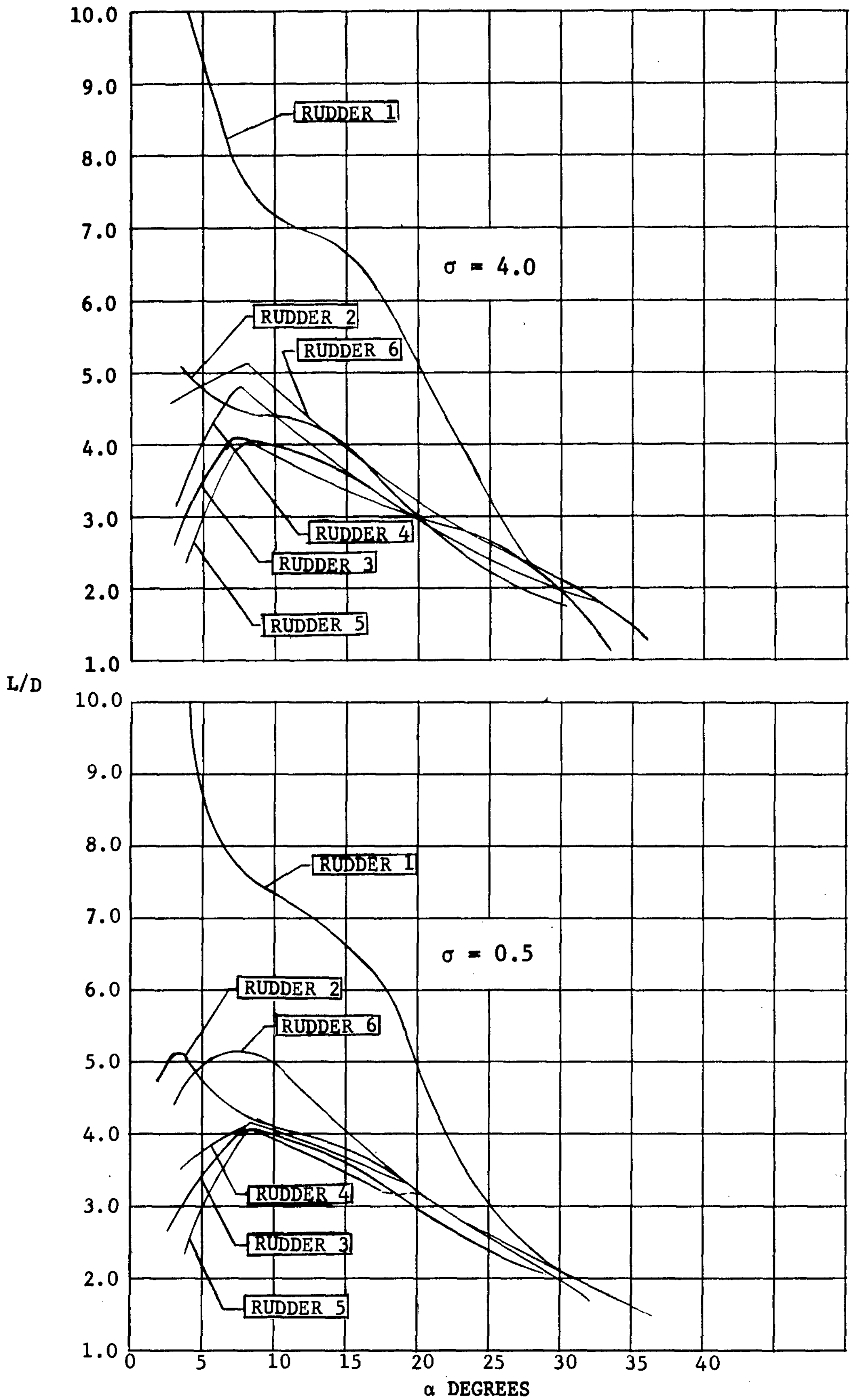


Figure 21 - Comparison of the Lift to Drag Ratios of the Rudders at Cavitation Indices of 4.0 and 0.5

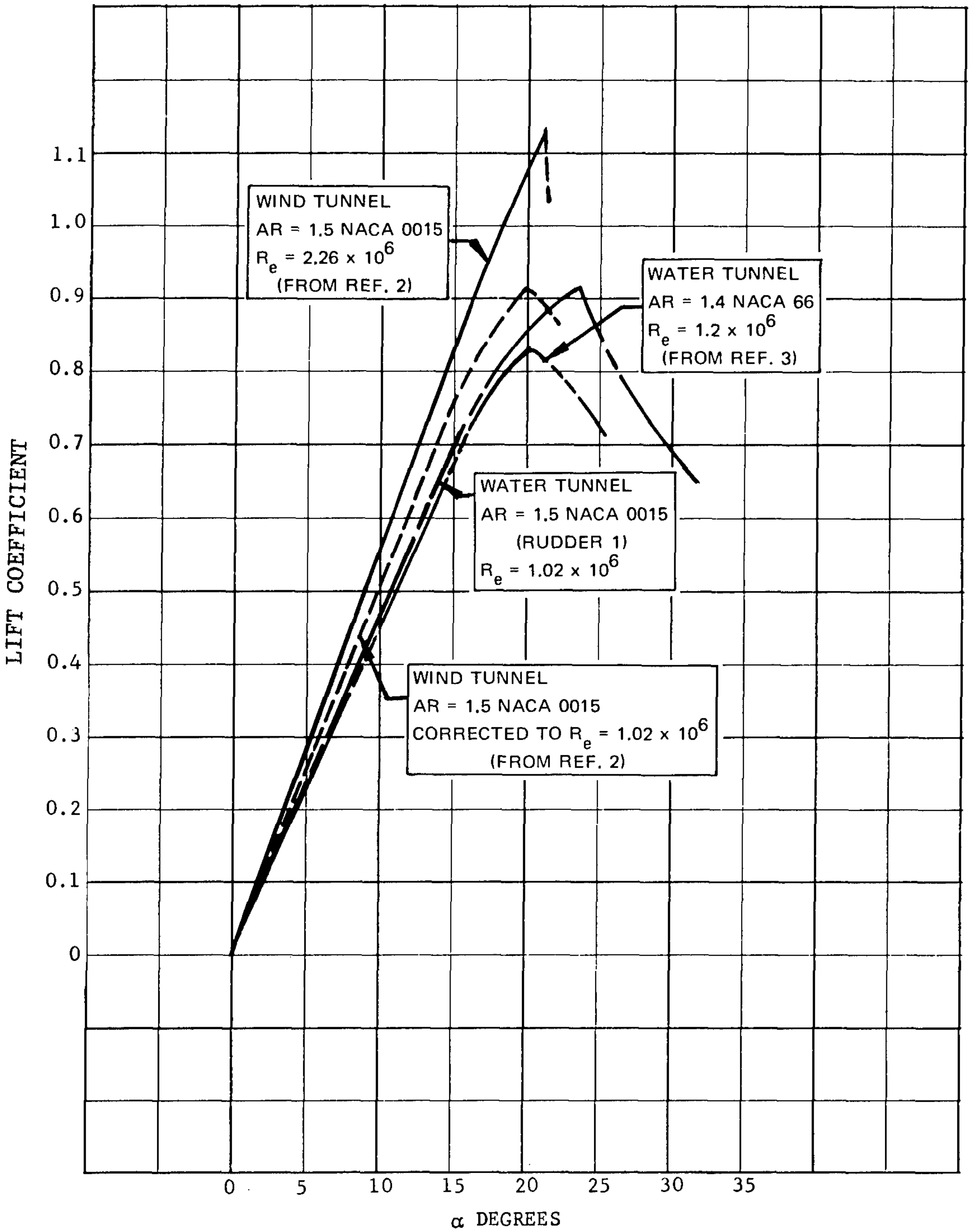


Figure 22 - Comparison of Lift Coefficient versus Angle of Attack for Rudder 1 as Determined from Wind Tunnel and Water Tunnel Experiments

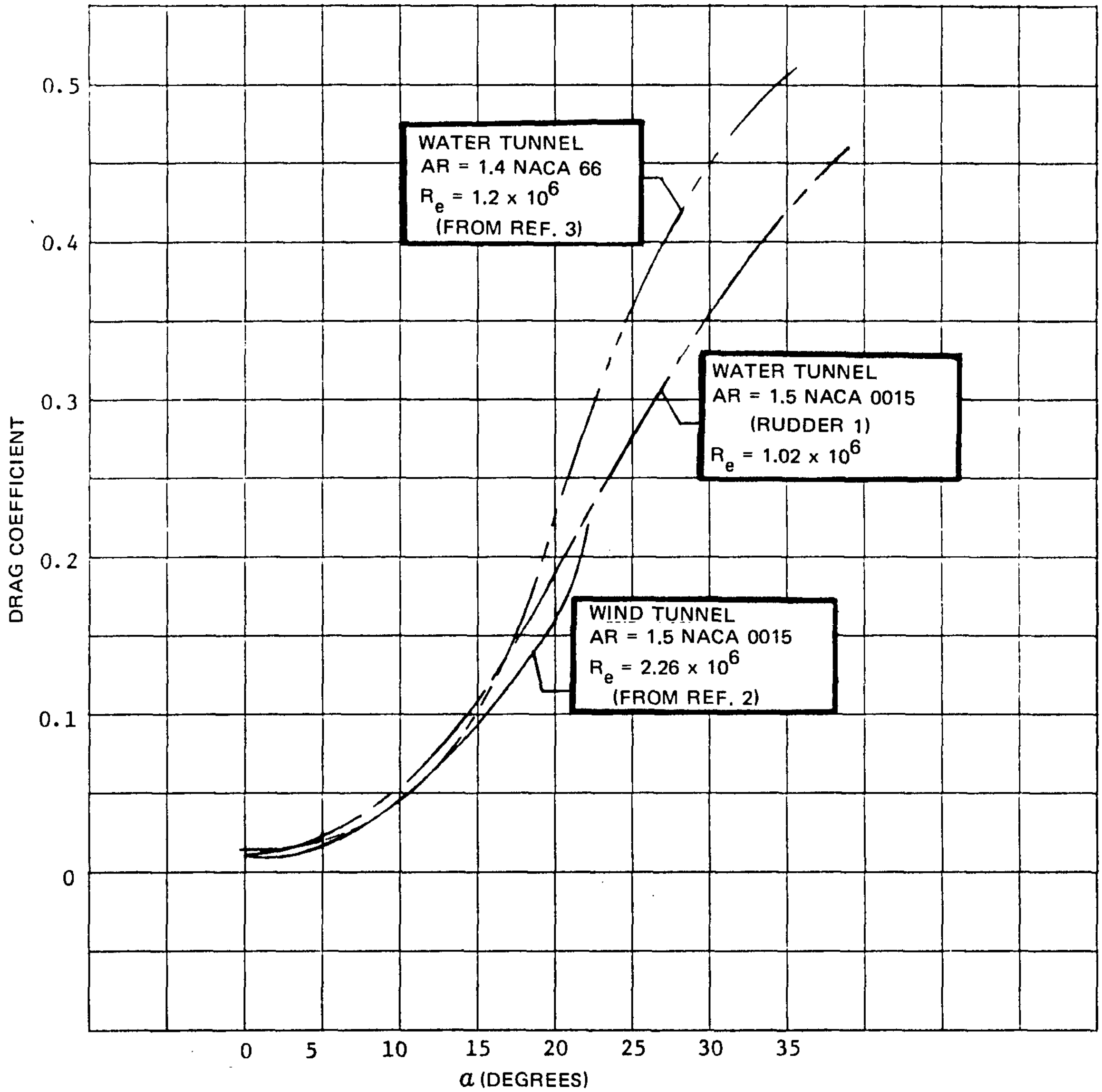


Figure 23 - Comparison of Drag Coefficient versus Angle of Attack for Rudder 1 as Determined from Wind Tunnel and Water Tunnel Experiments

INITIAL DISTRIBUTION
REPORT 4150

| SERIAL | |
|---|---|
| 1 | WES/LIBRARY |
| 2 | CHONR 438 |
| 3 | ONR BOSTON |
| 4 | ONR CHICAGO |
| 5 | ONR PASADENA |
| 6 | NRL 2627 LIB |
| 7 | USNA LIB |
| 8 | NAVPGSCOL LIB |
| 9 | NROTC & NAVADMINU, MIT |
| 10 | NAVWARCOL |
| 11 | SHIPS 2052 |
| 12 | SHIPS 03412/PETERSON |
| 13 | SHIPS 0372 |
| 14 | FAC 032C |
| 15 | ORD 035/SEIDMAN |
| 16 | NAVOCEANO 1640 |
| 17 | NAVAIRDEVCEN ADL |
| 18 | NELC LIB |
| 19 | NAVWPNSCEN |
| 20 | NAVUSEACEN SAN DIEGO |
| 21 | NAVUSEACEN 6005/FABULA |
| 22 | NAVUSEACEN PASADENA |
| 23 | NAVUSEACEN 2501/HOYT |
| 24 | CIVENGRLAB L31 LIB |
| 25 | NOL |
| 26 | NWL LIB |
| 27 | NPTLAB NUSC |
| 28 | NLONLAB NUSC |
| 29 | NAVSHIPYD BREM/LIB |
| 30 | NAVSHIPYD BSN/LIB |
| 31 | NAVSHIPYD CHASN/LIB |
| 32 | NAVSHIPYD HUNTERS PT/LIB |
| 33 | NAVSHIPYD LBEACH/LIB |
| 34 | NAVSHIPYD MARE/LIB |
| 35 | NAVSHIPYD MARE 250 |
| 36 | NAVSHIPYD PEARL/LIB |
| 37 | NAVSHIPYD PHILA 240 |
| 38 | NAVSHIPYD PTSMH/LIB |
| 39 | SEC 6034B |
| 40 | SEC 6110 |
| 41 | SEC 6114H |
| 42 | SEC 6120 |
| 43 | SEC 6136 |
| 44 | SEC 6140B/FONCANNON |
| 45 | SEC 6144G |
| 46 | SEC 6148 |
| 47 | SEC 6660.03/BLOUNT NORVA |
| 48 | AFOSR/NAM |
| 49 | DDC |
| 50 | DDC |

| SERIAL | |
|---|---|
| 51 | DDC |
| 52 | DDC |
| 53 | DDC |
| 54 | DDC |
| 55 | DDC |
| 56 | DDC |
| 57 | DDC |
| 58 | DDC |
| 59 | DDC |
| 60 | DDC |
| 61 | LC/SCI & TECH DIV |
| 62 | MMA LIB |
| 63 | MMA/MARITIME RES CEN |
| 64 | DOT LIB |
| 65 | U BRIDGEPORT/URAM |
| 66 | U CAL BERKELEY/DEPT NAME |
| 67 | U CAL NAME/PAULLING |
| 68 | U CAL NAME/WEBSTER |
| 69 | U CAL NAME/WEHAUSEN |
| 70 | U CAL SCRIPPS LIB |
| 71 | CIT AERO LIB |
| 72 | CIT/ACOSTA |
| 73 | CIT/WU |
| 74 | CATHOLIC U/HELLER |
| 75 | COLORADO STATE U ENGR RES CEN |
| 76 | CORNELL U/SEARS |
| 77 | FLORIDA ATLANTIC U OE LIB |
| 78 | FLORIDA ATLANTIC U/DUNNE |
| 79 | U HAWAII/BRETSCHNEIDER |
| 80 | U IOWA INST HYDR RES LIB |
| 81 | U IOWA IHR/KENNEDY |
| 82 | U IOWA IHR/LANDWEBER |
| 83 | LEHIGH U FRITZ ENGR LAB LIB |
| 84 | LONG ISLAND U/PRICE |
| 85 | MIT OCEAN ENGR LIB |
| 86 | MIT OCEAN ENGR/ABKOWITZ |
| 87 | MIT OCEAN ENGR/MANDEL |
| 88 | MIT OCEAN ENGR/NEWMAN |
| 89 | U MICHIGAN NAME LIB |
| 90 | U MICHIGAN NAME/COUCH |
| 91 | U MICHIGAN NAME/HAMMITT |
| 92 | U MICHIGAN NAME/OGILVIE |
| 93 | U MICHIGAN WILLOW RUN LABS |
| 94 | U MINNESOTA SAFHL/KILLEN |
| 95 | U MINNESOTA SAFHL/SCHIEBE |
| 96 | U MINNESOTA SAFHL/SONG |
| 97 | U MINNESOTA SAFHL/WETZEL |
| 98 | NOTRE DAME ENGR LIB |
| 99 | NOTRE DAME/STRANDHAGEN |
| 100 | SWRI APPLIED MECH REVIEW |

| SERIAL | |
|---|---|
| 101 | SWRI/ABRAMSON |
| 102 | STANFORD U CIV ENGR LIB |
| 103 | STANFORD U/STREET |
| 104 | STANFORD RES INST LIB |
| 105 | SIT DAVIDSON LAB LIB |
| 106 | SIT DAVIDSON LAB/BRESLIN |
| 107 | SIT DAVIDSON LAB/TSAKONAS |
| 108 | U WASHINGTON APL LIB |
| 109 | WEBB INST/LEWIS |
| 110 | WEBB INST/WARD |
| 111 | WHOI OCEAN ENGR DEPT |
| 112 | WPI ALDEN HYDR LAB LIB |
| 113 | SNAME |
| 114 | BETHLEHEM STEEL NEW YORK/LIB |
| 115 | BETHLEHEM STEEL SPARROWS |
| 116 | BOLT BERANEK AND NEWMAN LIB |
| 117 | EASTERN RES GROUP |
| 118 | ESSO DES DIV |
| 119 | GEN DYN ELEC BOAT/BOATWRIGHT |
| 120 | GIBBS & COX |
| 121 | HYDRONAUTICS LIB |
| 122 | HYDRONAUTICS/GERTLER |
| 123 | LOCKHEED M&S/WAID |
| 124 | DOUGLAS AIRCRAFT/SMITH |
| 125 | NEWPORT NEWS SHIPBUILDING LIB |
| 126 | NIELSEN ENGR/SPANGLER |
| 127 | NAR SPACE/UJIHARA |
| 128 | OCEANICS/ |
| 129 | SPERRY SYS MGMT LIB |
| 130 | SUN SHIPBUILDING AERO/HYDRO |
| 131 | ROBERT TAGGART |
| 132 | TRACOR |

## CENTER DISTRIBUTION

| SERIAL | | | |
|---|---|---|---|
| 133 | C | 1500 | CUMMINS WILLIAM E |
| 134 | C | 1502 | STUNTZ GEORGE R JR |
| 135 | C | 1520 | WERMTER RAYMOND |
| 136 | C | 1524 | WILSON CHARLES J |
| 137 | C | 1524 | WILSON CHARLES J |
| 138 | C | 1532 | DOBAY GABOR F |
| 139 | C | 1532 | GREGORY DOUGLAS L |
| 140 | C | 1540 | MORGAN WILLIAM B |
| 141 | C | 1560 | HADLER JACQUES B |
| 142 | C | 1572 | OCHI MARGARET D |

**DOCUMENT CONTROL DATA - R & D**

*(Security classification of title, body of abstract and indexing annotation must be entered when the overall report is classified)*

1. ORIGINATING ACTIVITY (Corporate author)

Naval Ship Research and Development Center
Bethesda, Md. 20034

2a. REPORT SECURITY CLASSIFICATION

UNCLASSIFIED

2b. GROUP

3. REPORT TITLE

FORCE AND MOMENT CHARACTERISTICS OF SIX HIGH-SPEED RUDDERS FOR USE ON HIGH-PERFORMANCE CRAFT

4. DESCRIPTIVE NOTES (Type of report and inclusive dates)

5. AUTHOR(S) (First name, middle initial, last name)

Douglas L. Gregory

| 6. REPORT DATE | 7a. TOTAL NO. OF PAGES | 7b. NO. OF REFS |
|---|---|---|
| November 1973 | 39 | 3 |

8a. CONTRACT OR GRANT NO.
Program Element 62512N
b. PROJECT NO. F35421
Subproject SF 35421006
c. Work Unit 1532-100
d.

9a. ORIGINATOR'S REPORT NUMBER(S)

4150

9b. OTHER REPORT NO(S) (Any other numbers that may be assigned this report)

10. DISTRIBUTION STATEMENT

APPROVED FOR PUBLIC RELEASE: DISTRIBUTION UNLIMITED

11. SUPPLEMENTARY NOTES

12. SPONSORING MILITARY ACTIVITY

Naval Ship Systems Command
Code 03412B

13. ABSTRACT

Six rudders with a geometric aspect ratio of 1.5 and widely varying section shapes were constructed to determine the effect of section shape on the cavitating performance of high-speed rudders. Experiments were conducted in the 24-in. variable-pressure water tunnel at cavitation indices between 4.0 and 0.5 and an angle of attack range from -5 to +35 deg. Section shape had little effect on the lift curve slope or on the maximum lift coefficient. However, the blunt base sections had substantially higher drag coefficients throughout the normal operating range of rudder angles. Rudder stock torque was significantly affected by section shape and cavitation index.

| 14 KEY WORDS | LINK A | | LINK B | | LINK C | |
|---|---|---|---|---|---|---|
| | ROLE | WT | ROLE | WT | ROLE | WT |
| High-Performance Craft | | | | | | |
| Rudder Forces under Cavitating Conditions | | | | | | |
| Water Tunnel Data | | | | | | |
| Wind Tunnel Data | | | | | | |